The Abdus Salam
International Centre
for Theoretical Physics

United Nations
Educational, Scientific and
Cultural Organization

IAEA
International Atomic Energy Agency

2370-1

School and Training Course on Dense Magnetized Plasma as a Source of Ionizing Radiations, their Diagnostics and Applications

8 - 12 October 2012

Introduction to Plasma Spectroscopy

H.-J. Kunze

Institute for Experimental Physics V
Ruhr-University, 44780
Bochum
Germany

Strada Costiera, 11 - 34151 - Trieste - Italy • Tel. +39 0402240111 • Fax. +39 040224163 • sci_info@ictp.it • www.ictp.it
ICTP is governed by UNESCO, IAEA, and Italy, and it is a UNESCO Category 1 Institute

Introduction to Plasma Spectroscopy

H.-J. Kunze

Institute for Experimental Physics V, Ruhr-University,
44780 Bochum, Germany

School and Training Course on Dense Magnetized Plasma
as a Source of Ionizing Radiations,
their Diagnostics and Applications

ICTP, Trieste, October 8 -12, 2012

Plasmas emit electromagnetic radiation, which contains information on the plasmas

Typical Spectrum

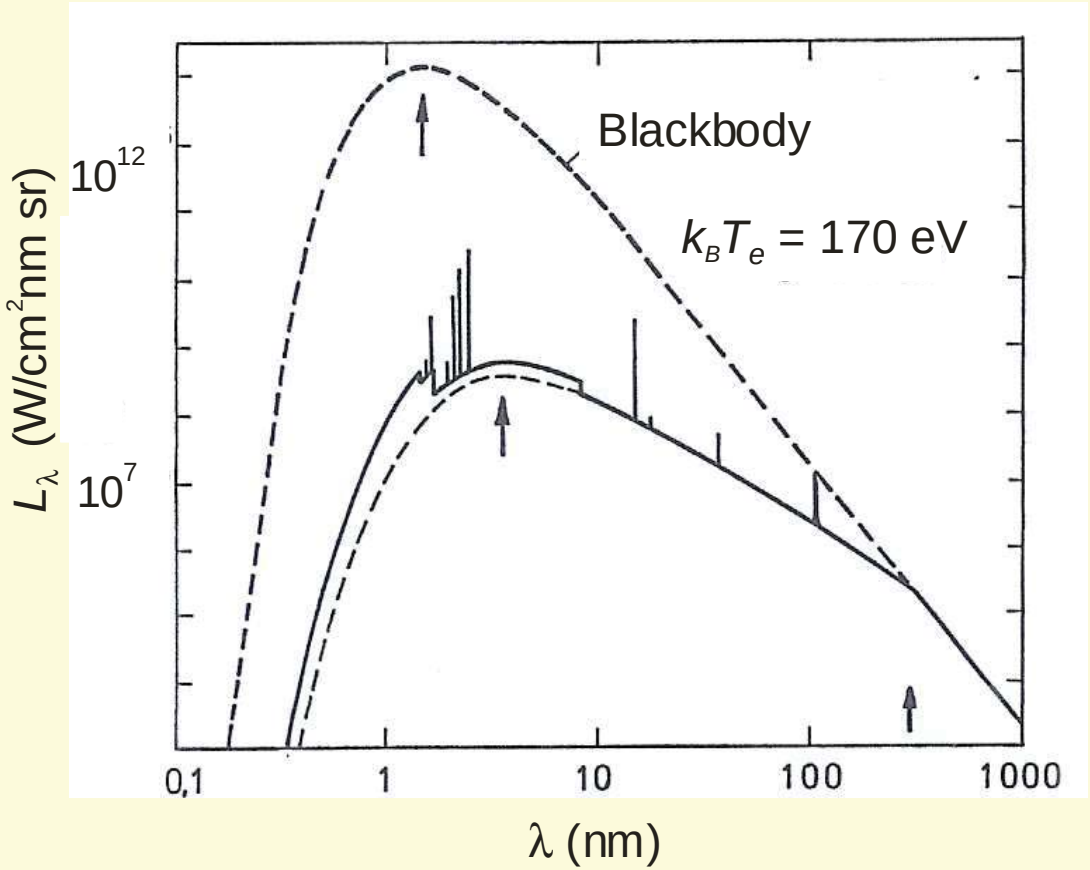

Continuum radiation

bremsstrahlung — free-free transitions

recombination radiation — free-bound transitions

Line radiation — bound-bound transitions

Energy levels of an atom or ion

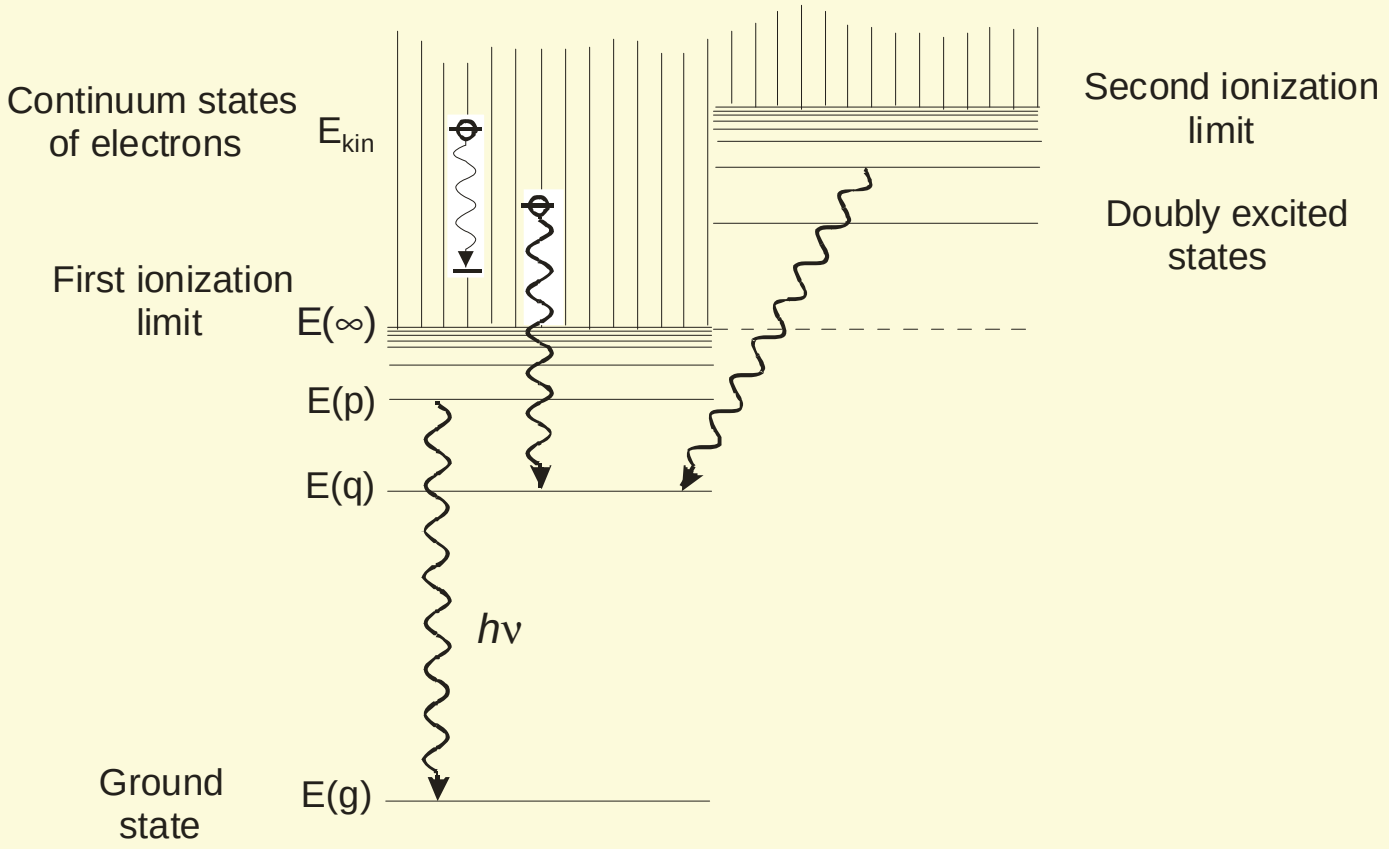

bremsstrahlung free-free transitions

recombination radiation free-bound transitions

line radiation bound-bound transitions

Maximum of bremsstrahlung emission

$$\frac{\lambda_{max}}{\text{nm}} \times \frac{kT_e}{\text{eV}} = 620$$

$kT_e = 100$ eV $\Rightarrow$ $\lambda_{max} = 6.2$ nm $\Rightarrow$ soft x-ray region

Line radiation from ions

present in even in pure hot hydrogen or deuterium plasmas (from walls or deliberately added for *diagnostics* or for *radiation cooling*, sometimes done in fusion devices)

50% of light or medium heavy elements with nuclear charge $6 \le Z_n \le 26$ are completely ionized for

$$\frac{kT_e}{\text{eV}} \ge 0.27\, Z_n^{3.4}$$

Examples: Ar $(Z_n = 18) \rightarrow kT_e \ge 5$ keV

C $(Z_n = 6) \rightarrow kT_e \ge 120$ eV

Local quantity which characterizes emission

Spectral emission coefficient $\varepsilon_\lambda,\ \varepsilon_\nu,\ \varepsilon_\omega$

defined by

$$\varepsilon_\lambda(\vec{r},\lambda) = \frac{\mathrm{d}^3\Phi}{\mathrm{d}V\ \mathrm{d}\Omega\ \mathrm{d}\lambda}, \quad \text{i.e.} \quad \text{unit} \quad \frac{\mathrm{W}}{\mathrm{m}^3\ \mathrm{sr\ nm}}$$

Φ is the flux out of the volume element dV

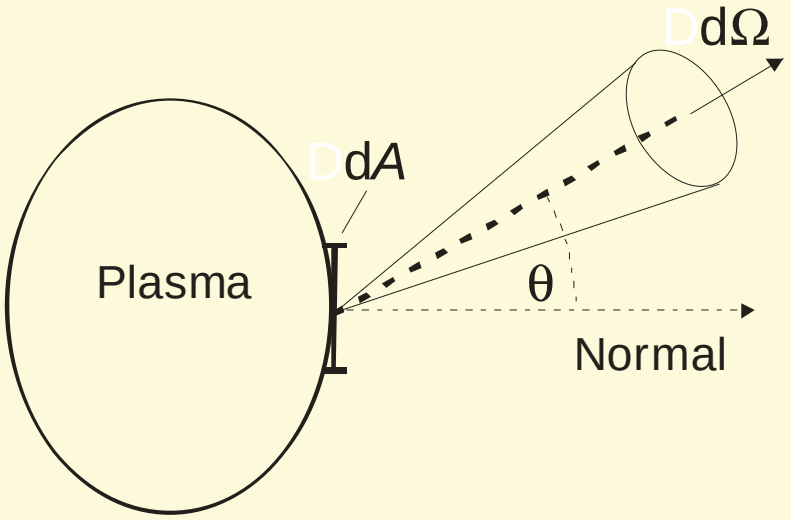

Observation:
Emission from the surface is a flux

Spectral radiance L_λ

(*Intensity !*)

$$L_\lambda = \frac{\mathrm{d}^2\Phi_\lambda}{\mathrm{d}A\cos\theta\,\mathrm{d}\Omega} \qquad \text{unit} \qquad \frac{\mathrm{W}}{\mathrm{m}^2\ \mathrm{sr\ nm}}$$

How does the flux, respectively the radiance, change through the plasma ?

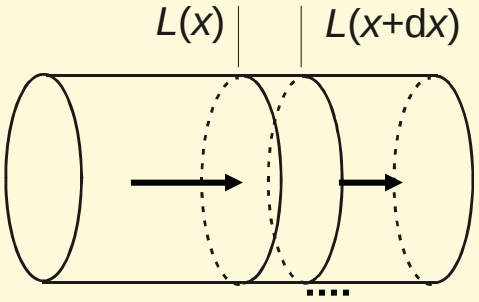

$$\mathrm{d}L_\lambda(x,\lambda) = \varepsilon_\lambda(x,\lambda)\,\mathrm{d}x - \kappa(x,\lambda)L_\lambda(x,\lambda)\,\mathrm{d}x$$

emission absorption

Optical depth $\mathrm{d}\tau = -\kappa(x,\lambda)\,\mathrm{d}x$ $\qquad \tau(x,\lambda) = -\int_0^x \kappa(x',\lambda)\,\mathrm{d}x'$

$$\frac{\mathrm{d}L_\lambda(x,\lambda)}{\mathrm{d}\tau} = L_\lambda(x,\lambda) - \frac{\varepsilon_\lambda(x,\lambda)}{\kappa(x,\lambda)} = L_\lambda(x,\lambda) - S_\lambda(x,\lambda)$$

Equation of radiative transfer

$S_\lambda(x,\lambda)$ source function

Low density plasmas
Hot plasmas

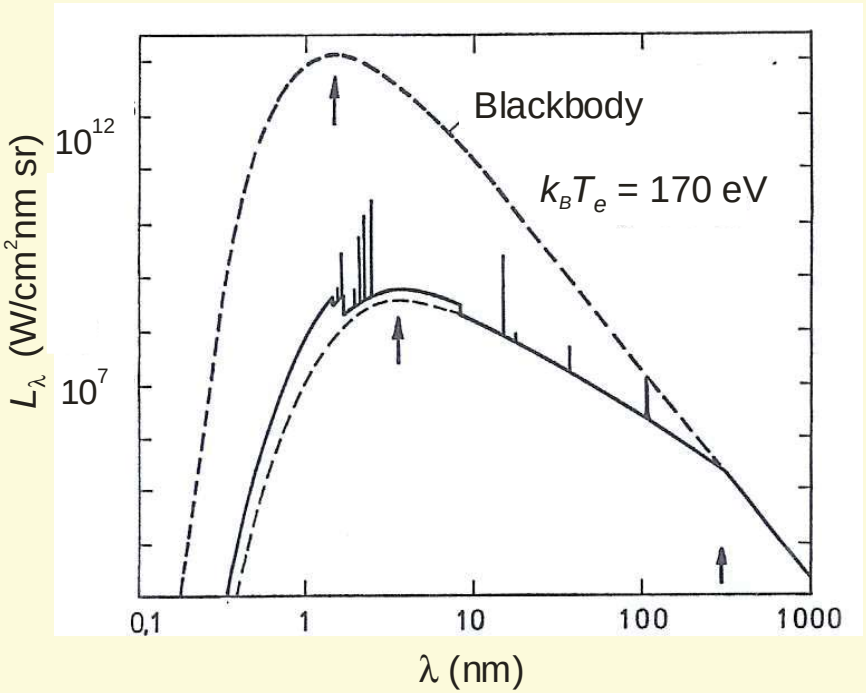

absorption negligible

Spectral radiance at the surface

$$x = 0$$

$$L_\lambda(0,\lambda) = \int_0^{\tau(-\ell,\lambda)} S_\lambda(\tau,\lambda)\,\mathrm{d}\tau$$

$$= \int_{-\ell}^{0} \varepsilon_\lambda(x,\lambda)\,\mathrm{d}x$$

Plasmas become optically thick first at long wavelength !

Lines $\tau(\lambda)$ μ $n(q)\,f$

lower state density × oscillator strength

resonance lines are most prone to absorption because of high n(q) !

$$L_\lambda(0,\lambda) = \int_{-\ell}^{0} \varepsilon_\lambda(x,\lambda)\,\mathrm{d}x$$

Drawback of *all* spectroscopic measurements

→ information along the line of sight

→ Computer tomography

measurements of the radiance in a large number of directions

(practically not possible in plasma devices)

Radial symmetry

Measurement of *L* along many chords

Abel inversion

Local values of $\varepsilon_\lambda(r,\lambda)$

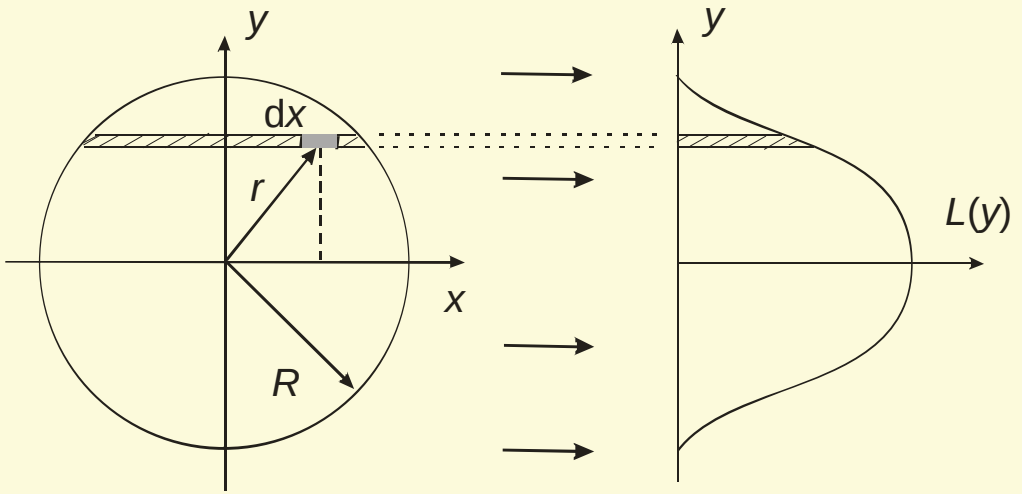

Applicable also to devices with one hole for the measurement

simple transformation

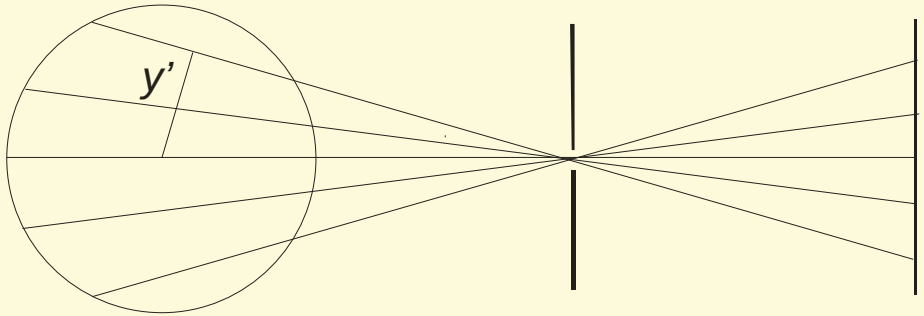

and to tokamaks with a limiter, where density contour lines are very close to a set of nested eccentric circles, the shift being known as Shafranov shift

and to plasmas with elliptic cross-section

(Rev. Sci. Instrum. **63**, 4757 (1992))

Distortion by a thick wall ?

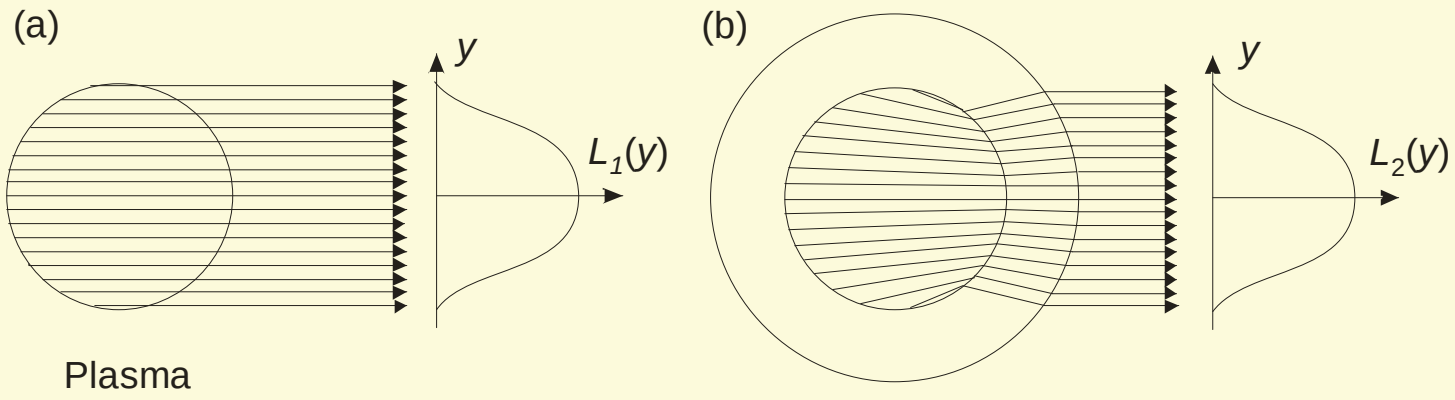

Reflection from the wall ?

(*Wavelength dependent*)

Can cause errors !!

Special case

Beam emission spectroscopy

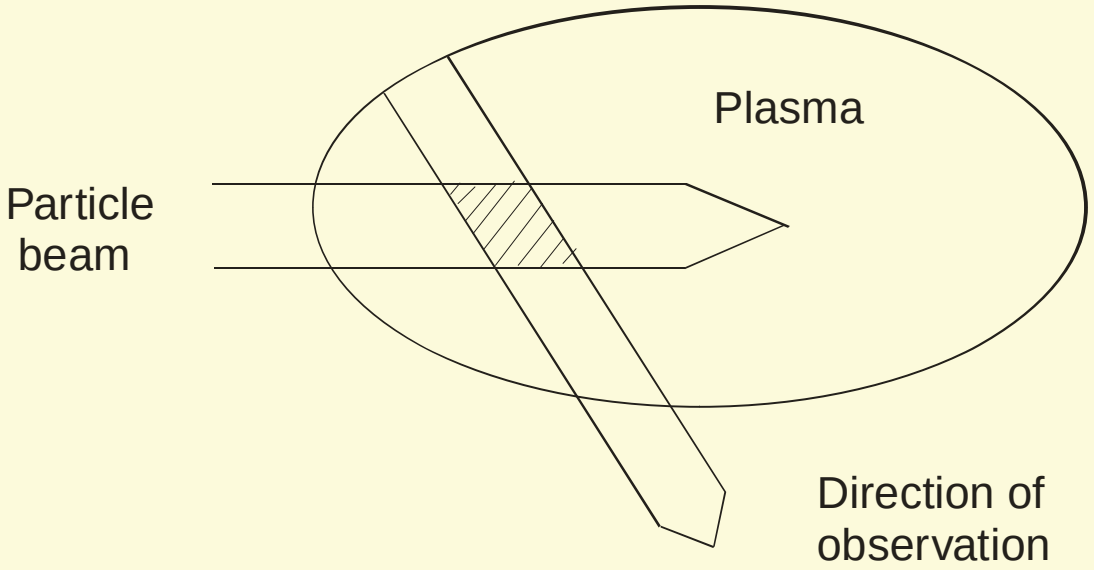

Local information

Li-beams → boundary diagnostics

He- beams

Li-beams (energetic) → magnetic field measurements

H-, D- beams → charge exchange spectroscopy

Let's now assume, we have the local spectral emission coefficient ε_λ in the plasma. What does it tell us?

Continuum radiation

Recombination radiation at long wavelengths becomes negligible

Bremsstrahlung at long wavelengths for a pure hydrogen plasma

$$\varepsilon_\lambda^{ff}(\lambda) \sim \frac{1}{\lambda^2} \frac{n_e^2}{(k_B T_e)^{1/2}}$$

Weak temperature dependence, strong electron density dependence → electron density diagnostics

With impurities:

$$\varepsilon_\lambda^{ff}(\lambda) \sim \frac{1}{\lambda^2} \frac{n_e \sum_{i,z} z_i^2 n_z^i}{(k_B T_e)^{1/2}}$$

All impurity ions of charge z contribute

Deviation of the emission coefficient from that of a pure H-plasma is a measure of the impurity contamination characterized in fusion plasmas by

$$\varepsilon_\lambda^{ff}(\lambda) = Z_{eff}\ \varepsilon_\lambda^{ff}(\lambda)(H)$$

Z_{eff} is some kind of a mean charge

At high densities plasmas become optically thick at long wavelengths → emission corresponds to that of a blackbody → temperature

At short wavelengths

both bremsstrahlung and recombination radiation

exponential dependence in frequency

$$\lg \varepsilon_\nu(\nu) \simeq \frac{1}{\ln 10}\,\frac{h\nu}{k_B T_e} + const$$

Slope of straight line gives T_e

Bremsstrahlung and Recombination radiation

$$e^{-\frac{h\nu}{k_B T_e}}$$

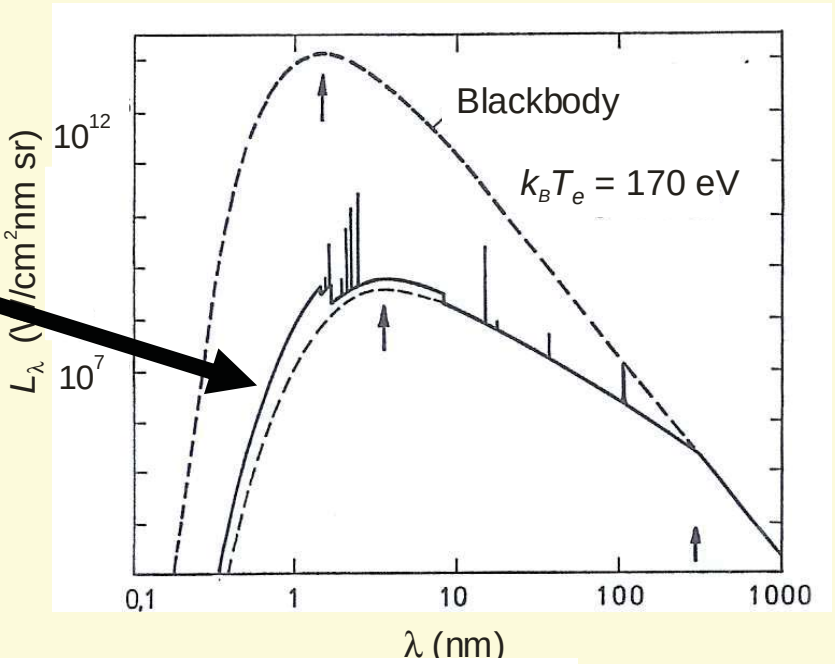

Examples

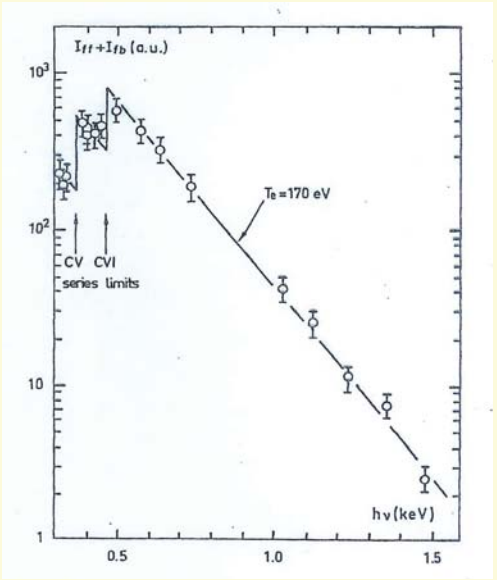

Laser-produced plasma

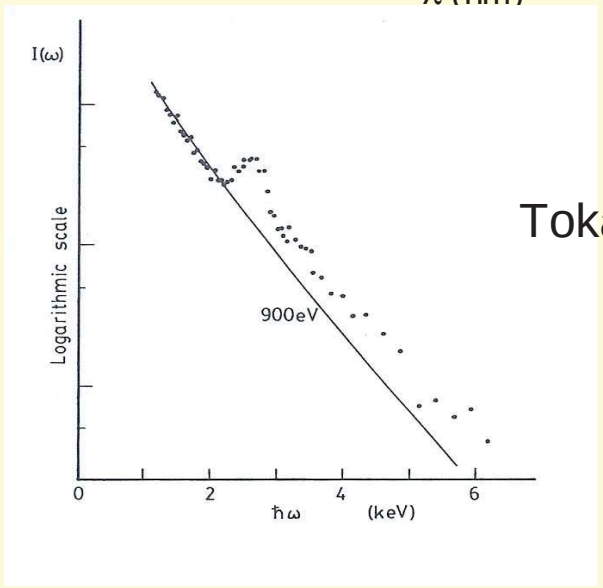

Tokamak

M. Galanti and N. J. Peacock
J. Phys. B **8**, 2427 (1975)

J. E. Rice, K. Molvig, H. I. Helava,
Phys. Rev. A **25**, 1645 (1982)

Line radiation

Emission coefficient of a line between upper level p and lower level q

$$\varepsilon(\nu) = \frac{h\nu}{4\pi} A(p \to q)\, n_z(p)$$

$A(p \to q)$ is the transition probability

The quantity obtained thus is the population density $n_z(p)$ of the upper level

Theoretical considerations are needed to establish how $n_z(p)$

is determined by the parameters of the plasma

General approach:

One identifies the relevant processes and sets up the appropriate system of rate equations

		Rate
radiative transitions	$A^{z+}(p) \rightarrow A^{z+}(q) + h\nu$	$A_z(p \rightarrow q)$
electron collisional transitions	$A^{z+}(q) + e^- \rightleftarrows A^{z+}(p) + e^-$	$n_e X_z(q \rightarrow p)$
electron collisional ionization	$A^{z+}(q) + e^- \rightarrow A^{(z+1)+}(g) + 2e^-$	$n_e S_z(p \rightarrow g)$
collisional recombination	$\neg$	$n_e^2 \alpha_{z+1}^{cr}(g \rightarrow p)$
radiative recombination	$A^{(z+1)+}(g) + e^- \rightarrow A^{z+}(q) + h\nu$	$n_e \alpha_{z+1}^{rr}(g \rightarrow p)$
dielectronic recombination	$A^{(z+1)}(g) + e^- \rightarrow A^{z+}(p^*)$	
	$\rightarrow A^{z+}(p) + h\nu$	$n_e \alpha_{z+1}^{dr}(g \rightarrow p)$

Proton collisions, photo-excitation and photo-ionization can be neglected in many cases although there are plasmas where they are important

$$\frac{\mathrm{d}n_z(p)}{\mathrm{d}t} = -\, n_z(p) \sum_{q \neq p} n_e X_z(p \to q) + \sum_{q \neq p} n_z(q)\, n_e X_z(q \to p)$$
$$- \, n_z(p) \sum_{q<p} A_z(p \to q) \quad + \sum_{r>p} n_z(r)\, A_z(r \to p)$$
$$- \, n_z(p)\, n_e S_z(p \to g) \quad + n_{z+1}(g)\, n_e^2\, \alpha^{cr}_{z+1}(g \to p)$$
$$+ n_{z+1}(g)\, n_e\, \alpha^{rr}_{z+1}(g \to p)$$
$$+ n_{z+1}(g)\, n_e\, \alpha^{dr}_{z+1}(g \to p)\,.$$

For the derivative of the ground state density $\frac{\mathrm{d}n_z(g)}{\mathrm{d}t}$ ionization from and recombination into levels of the lower ionization stage (z-1) should be added

X, S, and α are rate coefficients, *i.e.*

$$\langle \sigma v \rangle = \int \sigma\, v\, f_e(v)\mathrm{d}v$$

This means, that in some cases high energy tails of the distribution function may markedly influence population densities and may thus be detected, otherwise they depend on T_e

So, if one were to know all transition probabilities and all rate coefficients as function of T_e one should measure a spectrum as function of time, make a fit of the time dependent collisional radiative model to the observations, and one had the electron density n_e and the electron temperature T_e as function of time.

In general, this is still wishful thinking

However, in practice, simplifications are not only possible but even reasonable.

Looking at time scales allows first simplification in most cases:

Time scales of ionization and recombination are long compared to relaxation of excited level populations, which are at least given by 1/A.

One solves separately the rate equation of ionization/recombination

$$\frac{\mathrm{d}n_z(g)}{\mathrm{d}t} = -n_e n_z(g)\, S_z^{eff}(T_e, n_e) + n_e n_{z+1}(g)\, \alpha_{z+1}^{eff}(T_e, n_e)$$
$$+ n_e n_{z-1}(g)\, S_{z-1}^{eff}(T_e, n_e) - n_e n_z(g)\, \alpha_z^{eff}(T_e, n_e)$$

and

$$\frac{dn_z(p)}{dt} = 0 \quad for \quad p > g$$ *means*

Excited levels are in quasi-equilibrium with their ground states, they follow instantaneously their ground state density

Metastable levels ?

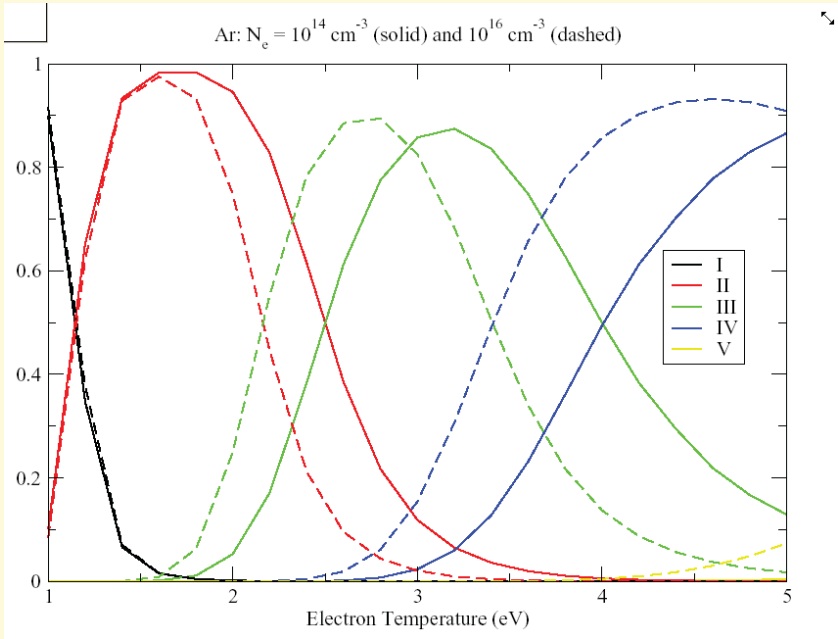

In stationary plasma

Distribution of ionization stages calculated for 2 densities:

Increasing density shifts Ionization to lower stages

Maximum abundance of an ion gives rough estimate of temperature at low densities

Simplification at low and high densities !

In *transient plasmas*: atoms go successively through their ionization stages till they reach equilibrium

$$\frac{\mathrm{d}n_z}{\mathrm{d}t} = n_\mathrm{e} S_{z-1} n_{z-1} - n_\mathrm{e} S_z n_z$$
$$+ n_\mathrm{e}(\alpha_{z+1}^{\mathrm{rr}} + \alpha_{z+1}^{\mathrm{dr}} + \alpha_{z+1}^{\mathrm{cr}}) n_{z+1} - n_\mathrm{e}(\alpha_z^{\mathrm{rr}} + \alpha_z^{\mathrm{dr}} + \alpha_z^{\mathrm{cr}}) n_z$$

In a rapidly ionizing plasma recombination is negligible

$$\frac{1}{n_z}\frac{\mathrm{d}n_z}{\mathrm{d}t} = n_\mathrm{e}\left(\frac{n_{z-1}}{n_z} S_{z-1} - S_z\right)$$

decaying part of the abundance $n_{z-1}/n_z \ll 1$

hence $$\frac{1}{n_z}\frac{\mathrm{d}n_z}{\mathrm{d}t} = -n_\mathrm{e} S_z$$

i.e. it reflects directly the ionization rate to the next ionization stage

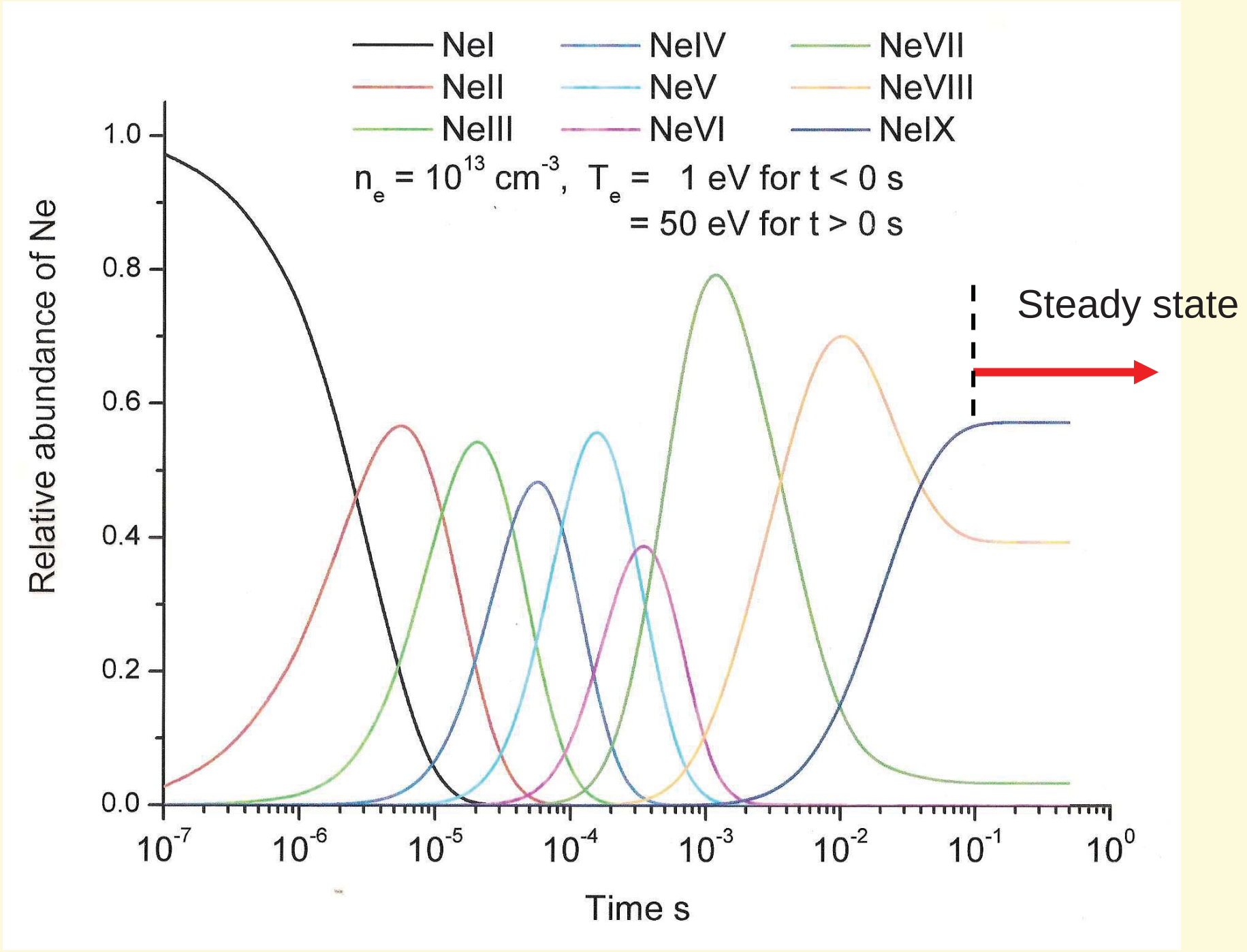
NeI
NeII
NeIII
NeIV
NeV
NeVI
NeVII
NeVIII
NeIX
$n_e = 10^{13}$ cm^{-3}, T_e = 1 eV for t < 0 s
= 50 eV for t > 0 s
Steady state
Relative abundance of Ne
1.0
0.8
0.6
0.4
0.2
0.0
10^{-7}
10^{-6}
10^{-5}
10^{-4}
10^{-3}
10^{-2}
10^{-1}
10^{0}
Time s

Dielectronic recombination

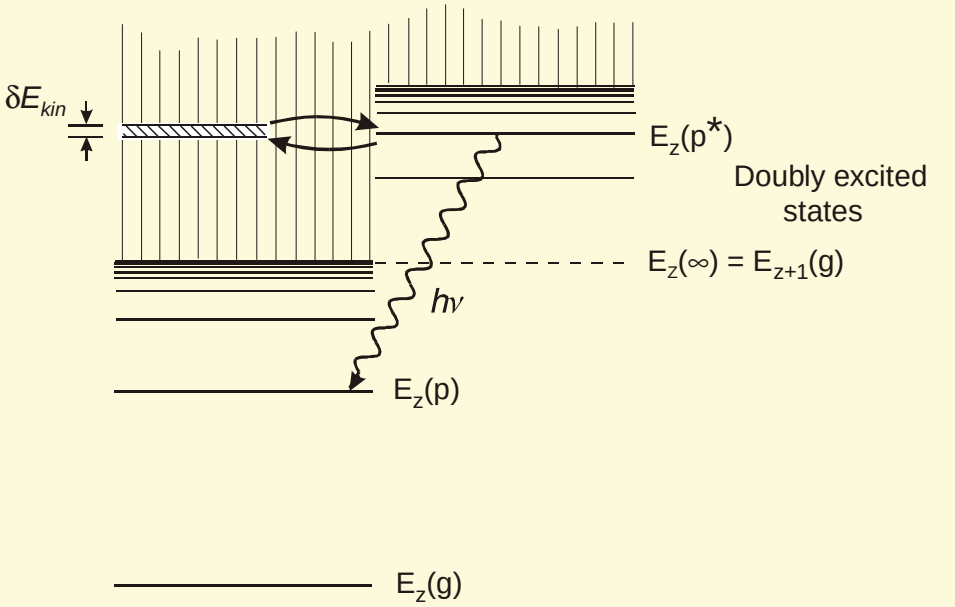

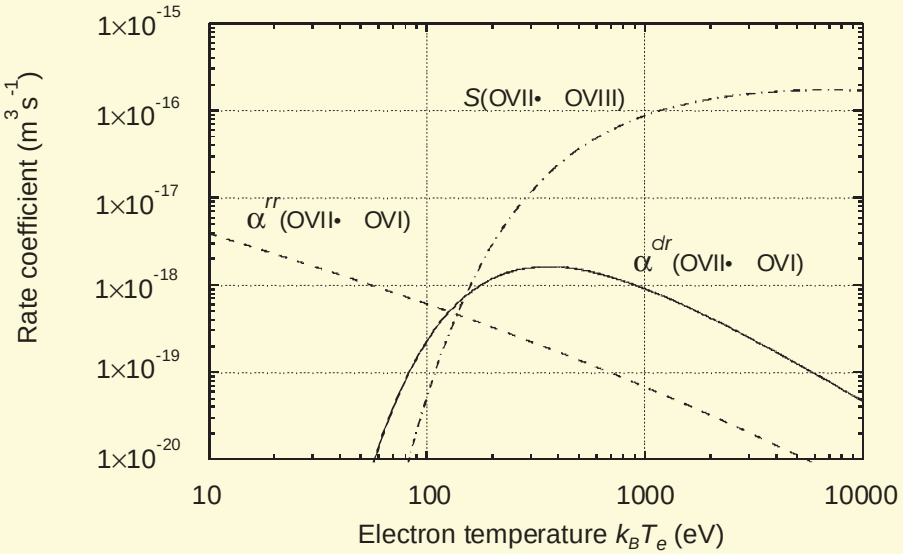

Dielectronic capture followed by a stabilizing transition (satellites !)

High densities: electron collisions dominate and establish a population equilibrium between the levels, which corresponds to that of thermodynamic equilibrium.
It is called local thermodynamic equilibrium (LTE)
(no equilibrium with the radiation field !!). *Explanation*!

Advantage: Equilibrium relations can be applied.

Boltzmann distribution:

$$\frac{n_z(p)}{n_z(q)} = \frac{g_z(p)}{g_z(q)} \exp\left[- \frac{E_z(p) - E_z(q)}{k_B T_e} \right]$$

Saha-Eggert equation:

$$\frac{n_{z+1}(g)\, n_e}{n_z(q)} = \frac{g_{z+1}(g)}{g_z(q)} \frac{1}{\lambda_B^3} \exp\left(- \frac{E_{z,q\infty}}{k_B T} \right) \qquad \text{mit} \qquad \lambda_B = \left(\frac{2\pi\hbar}{m_e k_B T} \right)^{1/2}$$

$$\frac{n_{z+1} n_e}{n_z} = 2 \frac{U_{z+1}(T)}{U_z(T)} \frac{1}{\lambda_B^3} \exp\left(- \frac{E_{z,g\infty}}{k_B T} \right)$$

$g_z(p)$ statistical weight of level (p) of ion (z)
$U_z(T)$ partition function of ion (z)
λ_B thermal deBroglie wavelength

With decreasing electron density collisional coupling ceases to exist first between levels with the largest energy separation, which in many cases is between ground state and excited state

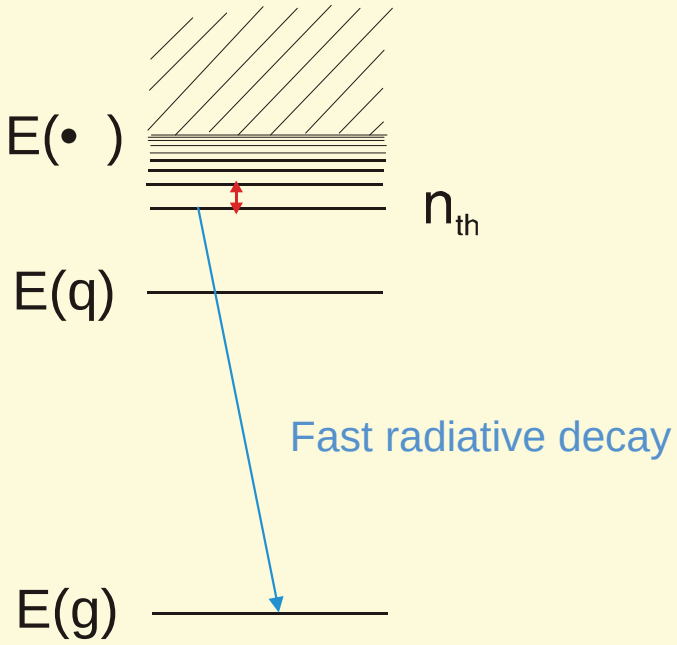

n_{th} thermal level

above n_{th} equilibrium relations still prevail

Partial local thermodynamic equilibrium (PLTE)

Low densities

$n_e X$ versus A

Collisional processes are weak, radiative ones dominate

Excitation of levels is typically from the ground state (maybe from a metastable state) by electron collisions, depopulation by radiative decay

$$n_z(g)\, n_e X(g \rightarrow p; T_e) = n_z(p)\, A(p \rightarrow)$$

$$n_z(p) = n_z(g)\, \frac{n_e X(g \rightarrow p; T_e)}{A(p \rightarrow)} = f(n_e, T_e)$$

Excited state populations are low, most ions are in the ground state or in a metastable state

Low density limit is also called corona approximation

Distribution of the ions at low densities:

$$n_z n_e S_z(T_e) = n_{z+1} n_e (\alpha^{rr}_{z+1} + \alpha^{dr}_{z+1})$$

$$\frac{n_{z+1}}{n_z} = \frac{S_z(T_e)}{\alpha^{rr}_{z+1}(T_e) + \alpha^{dr}_{z+1}(T_e)} = f(T_e)$$

known as corona distribution

Examples of spectroscopic methods

employing the fundamental equation

$$\varepsilon(p \to q) = \frac{h\nu_{pq}}{4\pi} A(p \to q)\, n_z(p)$$

$$n_z(p) = \frac{4\pi\, \varepsilon(p \to q)}{h\nu_{pq} A_z(p \to q)}$$

Particle densities n_z

At high densities with LTE satisfied for the ion:

$$n_z = \frac{n_z(p)}{g_z(p)} U_z(T_e) \exp\left[+\frac{E_z(p) - E_z(q)}{k_B T_e}\right]$$

$$= \frac{4\pi\, \varepsilon(p \to q)}{h\nu_{pq} A_z(p \to q)} \frac{U_z(T_e)}{g_z(p)} \exp\left[\frac{h\nu_{pq}}{k_B T_e}\right]$$

T_e and partition function $U_z(T_e)$ must be known to obtain n_z!

In case the upper level is in PLTE, the Saha Eggert equation yields

$$n_{z+1}(g) = \frac{4\pi\,\varepsilon_z(p \to q)}{h\nu_{pq} A_z(p \to q)} \frac{2g_{z+1}(g)}{g_z(p)} \frac{1}{n_e} \left(\frac{m_e k_B T_e}{2\pi\hbar^2} \right)^{3/2} \exp\left(- \frac{E_{z,p\infty}}{k_B T_e} \right)$$

Now also the electron density n_e must be known, in addition.

At low densities in the coronal regime

$$n_z \simeq n_z(g) = \frac{A_z(p \to)}{n_e X_z(g \to p)} n_z(p)$$

$$= \frac{4\pi\,\varepsilon_z(p \to q)}{h\nu_{pq} A_z(p \to q)} \frac{A_z(p \to q)}{n_e X_z(g \to p; T_e)}$$

Forbidden transitions of the M1-type between fine structure levels of the ground state of highly ionized atoms.

Electron and proton collisions are fast enough to establish equilibrium population distribution given simply by the statistical weigths
Thus one line suffices to calculate n_z,
neither n_e nor T_e must be known

Further advantage: lines of many ions are in the visible.

Examples are the green and red iron lines of FeXIV and FeXV observed first in the solar corona, now used in many tokamaks

Charge exchange with injected fast beams of hydrogen is an indispensable tool to measure the • -particles produced in a burning plasma (local).

$$n_z(p)\, A(p \rightarrow) = \langle \sigma^{cx}(v)\, v \rangle\, n_{z+1} n_b$$

Charge exchange is selectively into levels of high principal quantum number and there into high *l*, decay via $\Delta n_p = -1$ transitions at long wavelengths

Helium-like ions

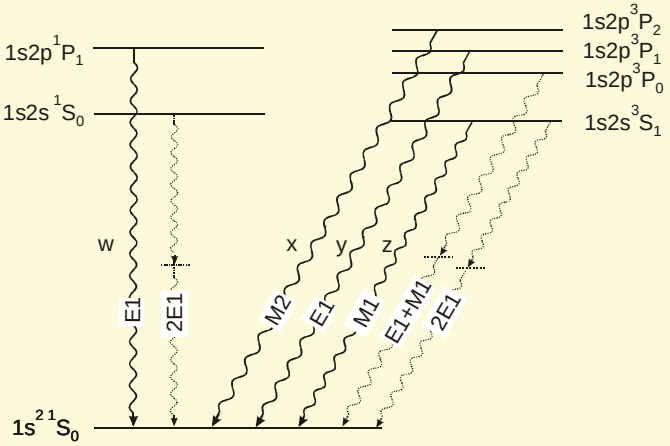

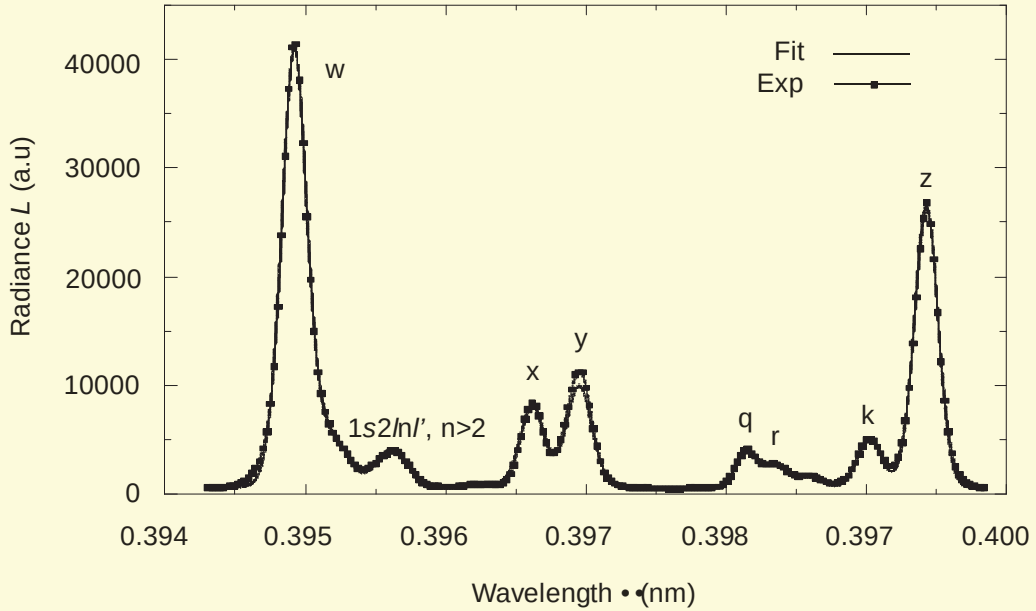

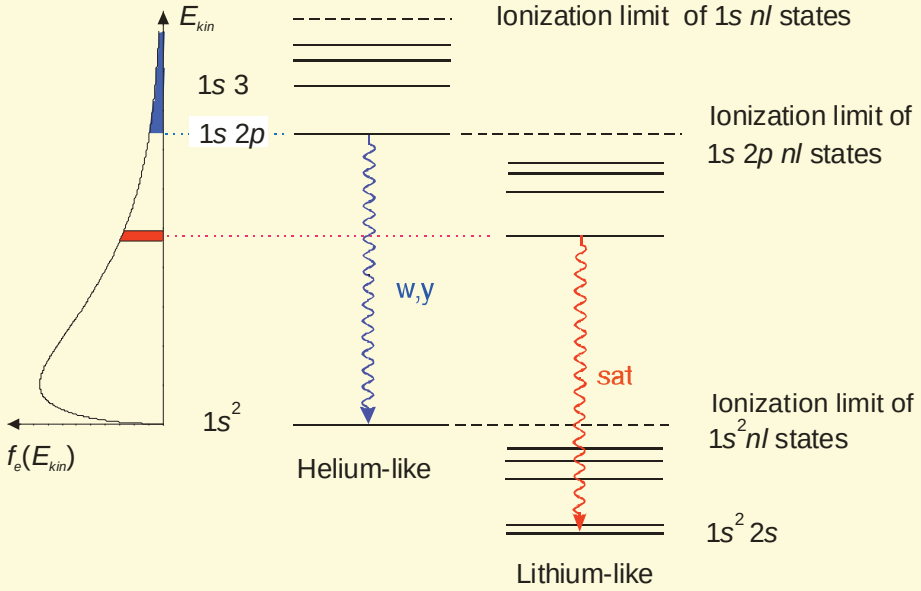

w: resonance line
y: intercombination line
x,z: forbidden lines

Dielectronic and innershell excited satellites

all close in wavelength

Resonance line: $\varepsilon_w \;\mu\; n_e\; X_w(T_e)\, n_{He}(g)$

Dielectronic satellite $\varepsilon_{sat}^{dr} \;\mu\; n_e\, \alpha_{He}^{dr}(T_e)\, n_{He}(g)$

Innershell excitation $\varepsilon_{sat}^{in} \;\mu\; n_e\; X^{in}(T_e)\, n_{Li}$

$$\frac{\varepsilon_{sat}^{dr}}{\varepsilon_w} = F_1(T_e)$$

$$\frac{\varepsilon_{sat}^{in}}{\varepsilon_w} \;\mu\; F_2(T_e)\, \frac{n_{Li}}{n_{He}}$$

The z-line is essentially populated by recombination of the hydrogenlike ion:

$$\frac{\varepsilon_z}{\varepsilon_w} \;\mu\; F_3(T_e)\, \frac{n_H}{n_{He}}$$

Such spectra of heavy helium-like ions are now much used in *tokamak plasmas (*up to Ni*)*. They are in the x-ray region.
Look at the nice fit of the previous example!!
They certainly are observed also in high-density hot plasmas

Electron temperature

One example for low densities we just have seen.

Taking line ratios is convenient since the ground state density and the electron density drop

$$\frac{\varepsilon_z(p \to q)}{\varepsilon_z(p' \to q')} = \frac{\lambda_{p'q'}}{\lambda_{pq}} \frac{A_z(p \to q)}{A_z(p' \to q')} \frac{A_z(p' \to)}{A_z(p \to)} \frac{X_z(g \to p)}{X_z(g \to p')} = f(T_e)$$

You need to know the excitation functions !

With increasing density, ratios become also dependent on the electron density and one has to use, in general, collisional-radiative models

Ratios become simple at high densities, when the upper level populations are described by a Boltzmann distribution
Check for condition !

$$\frac{\varepsilon_z(p \to q)}{\varepsilon_z(p' \to q')} = \frac{\lambda_{p'q'}}{\lambda_{pq}} \frac{A_z(p \to q)}{A_z(p' \to q')} \frac{g_z(p)}{g_z(p')} \exp\left[- \frac{E_z(p) - E_z(p')}{k_B T_e} \right]$$

Instead of several line pairs:

calculate the population densities $n_z(p)$ of the upper levels, and plot $\lg[n_z(p)]$ versus the energy $E_z(p)$

→ Boltzmann plot
straight line, the slope gives T_e

For high sensitivity energy separation of levels should be large !

Lines from successive ionization stages

For example: Saha-Eggert equation connects population of upper level (p') of ion (z) with population of ground state of ion (z+1), and Boltzmann relation connects that with the Population density $n_{z+1}(p)$ of level (p) in that ion

A number of examples are found in the literature.
Drawback: valid only in some high density range

Electron density

From line ratios

Select one line with an upper level (p) decaying essentially only by radiation to the ground state,
and another line where the upper level (p') is also depopulated by collisions

$$n_z(g)\, n_e\; X_z(g \to p) \simeq n_z(p)\, A(p \to)$$

$$n_z(g)\, n_e\, X_z(g \to p') \simeq n_z(p')\left[A(p' \to) + n_e X_z(p' \to)\right]$$

$$\frac{\varepsilon_z(p \to q)}{\varepsilon_z(p' \to q')} \cong \frac{\lambda_{p'q'}}{\lambda_{pq}} \frac{A_z(p \to q)}{A_z(p \to)} \frac{A_z(p' \to)}{A_z(p' \to q')} \frac{X_z(g \to p)}{X_z(g \to p')}$$

$$\times \left[1 + n_e \frac{X_z(p' \to)}{A_z(p' \to)}\right]$$

Example

Ratio of intercombination and resonance line in helium-like ions
(often used in laser-produced plasmas)

Further advantage: lines are close-by in wavelength!

Spectral lines are broadened
natural broadening
Doppler broadening
Stark broadening
van der Waals broadening
resonance broadening

$$\varepsilon_\lambda(\lambda) = \varepsilon(p \to q)\, \mathfrak{L}(\lambda)$$

$$\int_{-\infty}^{\infty} \mathfrak{L}(\lambda)\, \mathrm{d}\lambda = 1$$

$\mathfrak{L}(\lambda)$ line profile, line shape function

Natural broadening is typically negligibly small

Stark broadening (pressure broadening) is by charged plasma particles (electrons and ions). Their electric field leads to broadening of the levels.

Two approximations are usually employed to calculate the broadening. Very difficult to calculate in general, so this was to benefit of the experimentalists who had to furnish experimental verifications

Impact approximation and *quasistatic approximation*

Impact approximation: electric field produced by the electrons varies so rapidly at the position of the radiator, that the effect can be treated as collision.

In cases, where the broadening effect on the lower state can be neglected (one-state version), the half-width of a line is

$$\Delta\omega_{1/2} \cong n_{\mathrm{e}} X(\mathrm{p})$$

where X(p) stands for the sum of elastic and inelastic collisions.

Collisions with neighboring fine structure levels usually being strongest leads to

$$\Delta\omega_{1/2} \mu \frac{n_e}{(T_e)^x} \quad \textit{with} \quad 0.2 < x < 0.5$$

(weak temperature dependence)

Lines are also shifted! In principle, it also can be used for density diagnostics, but it is less accurate!

Broadening data (including the corrections by the ion contributions) are found in the book by Griem (Spectral Broadening by Plasmas, Academic Press, 1974)

A comprehensive bibliographic data bank is maintained at NIST

http://physics.nist.gov/cgi-bin/ASBib1/LineBroadBib.cgi

Profiles have a Lorentzian shape

Quasistatic approximation:

The field produced by the ions is considered static during the emission process. This microfield splits and shifts upper and lower levels by the Stark effect. Perturbation theory gives

$$\Delta\omega_{pq}(E) = C_{pq}^{k}\, E^{m},$$

where m=1 and m=2 holds for linear and quadratic Stark effect and (k) designates the Stark component. First calculation of the microfield was by Holtsmark, new calculations are mostly for high densities. The line profiles mirror the microfield distribution, certainly slightly modified by electron collision contributions

Because the linear Stark effect is much stronger than the quadratic Stark effect, the quasistatic approximation is appropriate for hydrogen and hydrogenic ions.

Theory is still being improved, and good measurements are needed for comparison

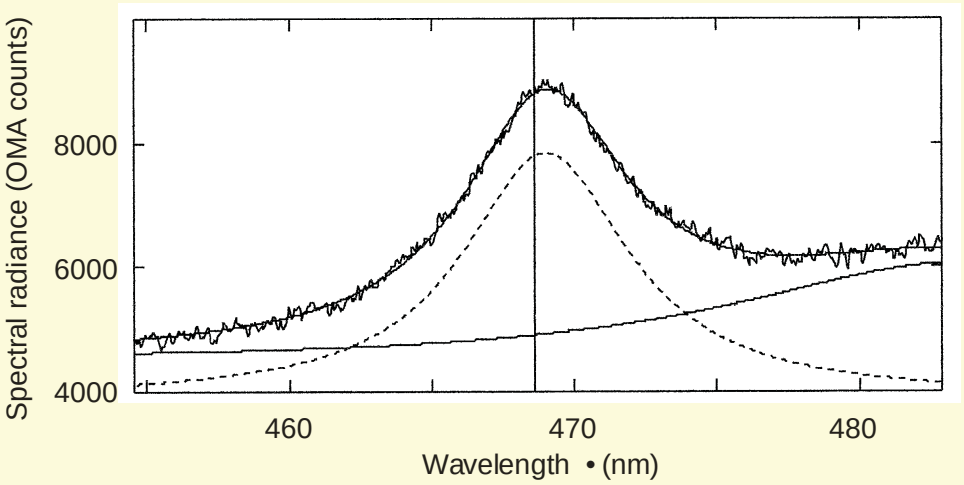

Paschen-α line of HeII at 468.6 nm measured for n_e= 3.5 x 10^{24} m^{-3} $k_B T_e$= 6.8 eV emitted from a well diagnosed pinch device

$$\frac{\Delta\lambda_{1/2}}{\text{nm}} \simeq 2.74\times10^{-20}\left(\frac{n_e}{\text{m}^{-3}}\right)^{0.831}$$

The most widely used line for density measurements is the H_β-line of hydrogen at 486.13nm with a central dip

With increasing principal quantum number n_p of upper levels lines become broader and finally merge Inglis Teller limit

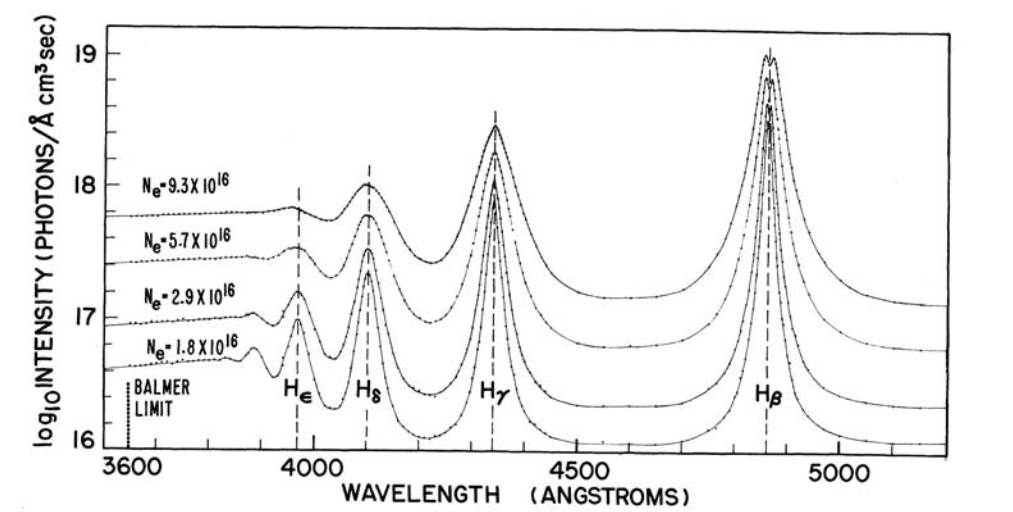

H Balmer series

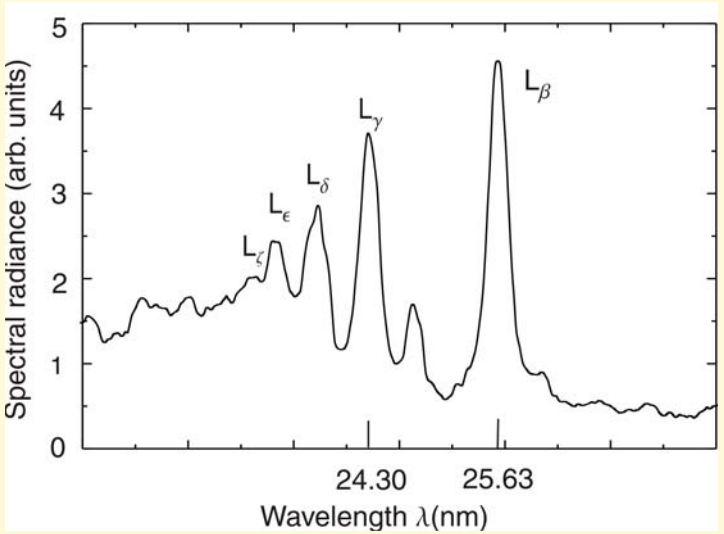

He Lyman series

Allows estimate of the perturber density

$$\lg \frac{n_z}{\mathrm{m}^{-3}} \approx 29.12 + 4.5 \lg Z - 1.5 \lg z - 7.5 \lg n_{p,\max}$$

Lines with forbidden components (e.g. HeI lines)

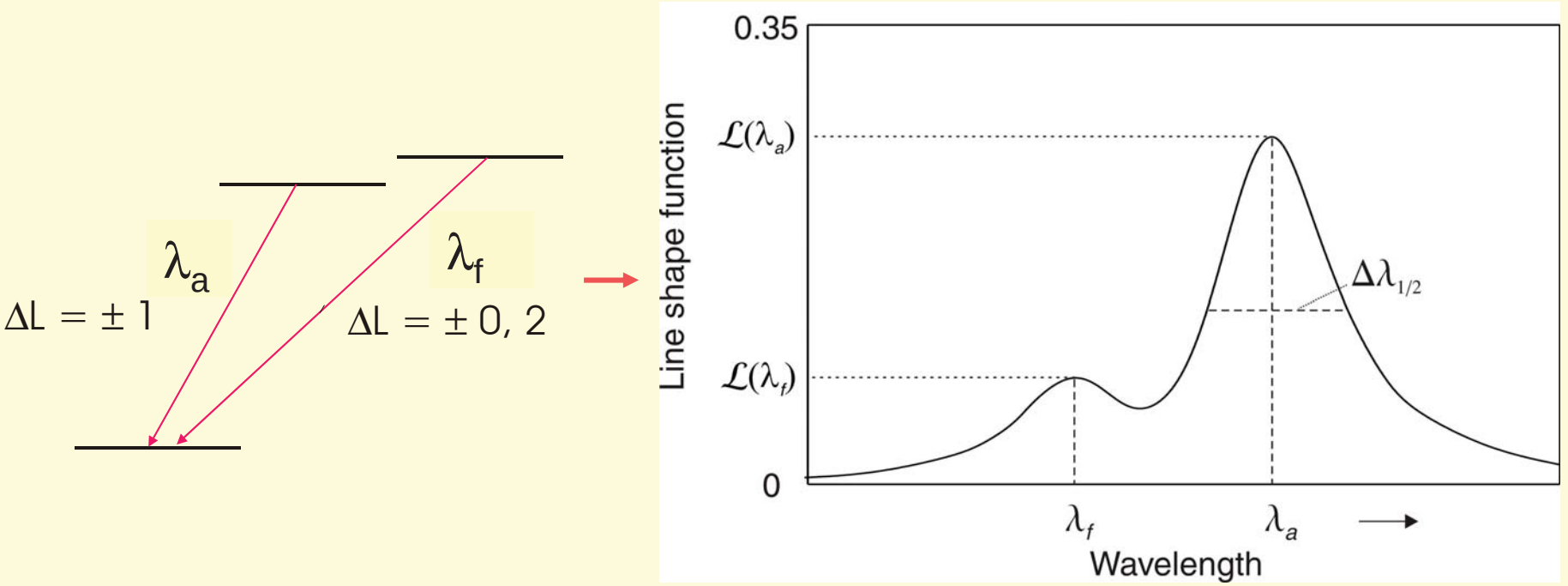

Electric field increasing with density mixes wave-functions of upper levels forbidden lines increase

When the self-absorption of a line becomes important
(the optical depth τ grows)

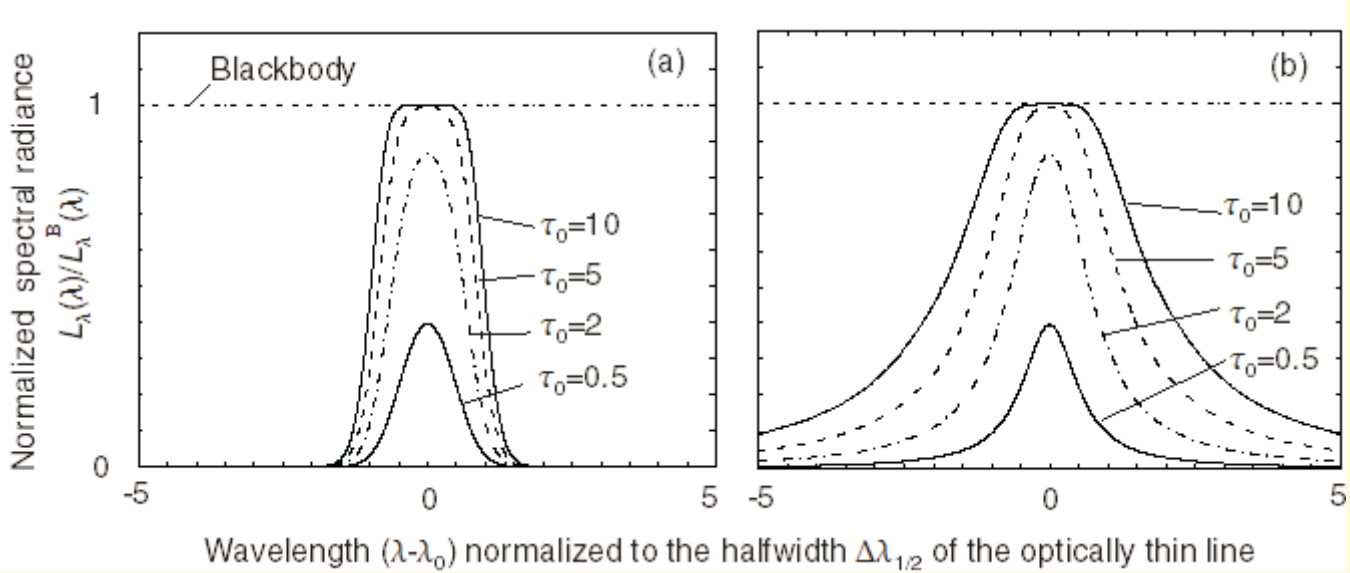

Flat maximum temperature measurement

In the wings, radiation can escape !

In the case of cooler boundary → self-reversal

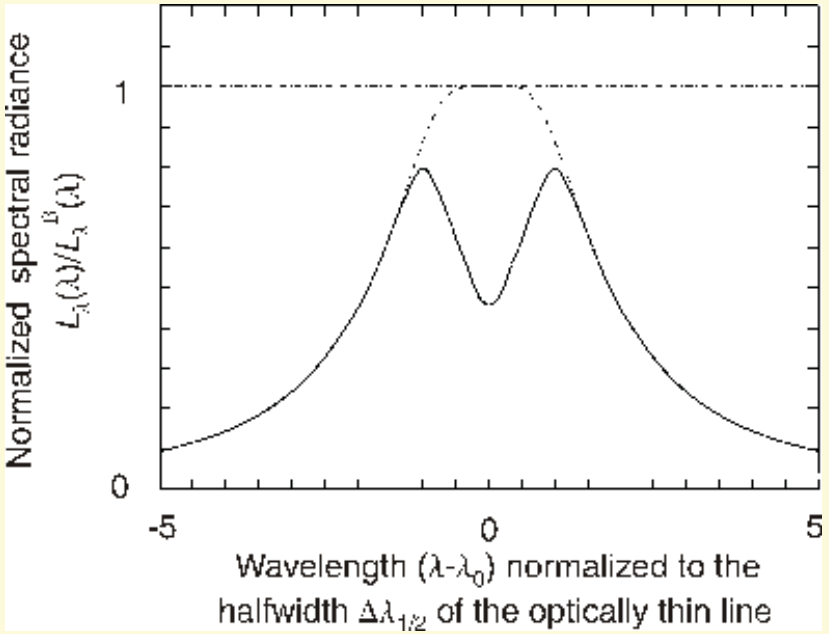

Transition 2p→2s
of CIV

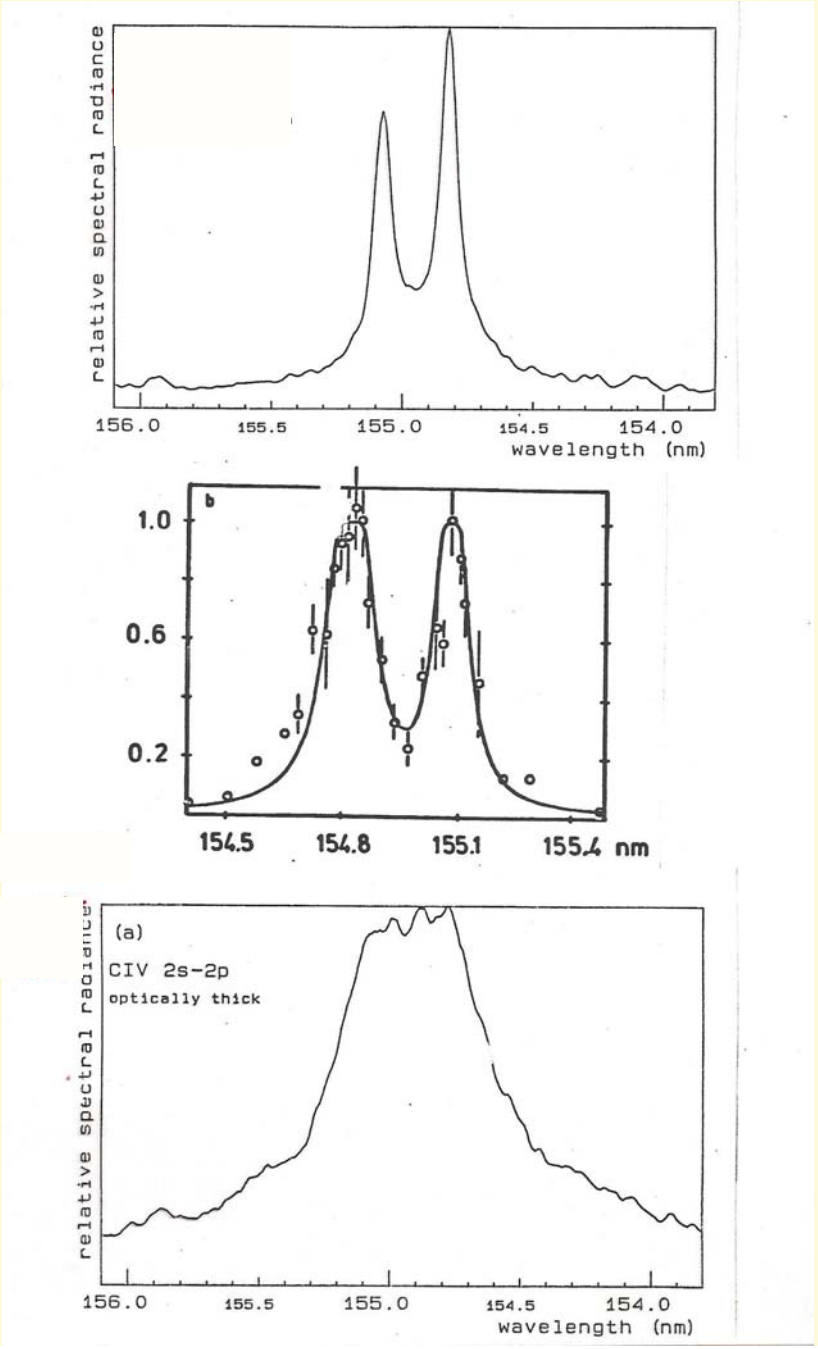

$$120\,000\ \mathrm{K}$$

$$L = 100\ \frac{\mathrm{kW}}{\mathrm{cm}^2}$$

Particle temperature T_z

Motion of an emitter results in Doppler shift of emitted lines

$$\frac{\omega - \omega_{pq}}{\omega_{pq}} = \frac{v_x}{c},$$

where v_x is the velocity component in the direction x of emission, and c is the speed of light.

Line profile and velocity distribution function are related by

$$\mathfrak{L}_{\mathrm{D}}(\omega)\,\mathrm{d}\omega = f_z(v_x)\,\mathrm{d}v_x$$

The line profile thus mirrors $f_z(v_x)$, and if this is Maxwellian, the profile has a Gaussian shape ⟶
half width gives T_z

$$\frac{\Delta\lambda_{1/2}}{\lambda_{pq}} = 7.715\times10^{-5}\sqrt{\frac{k_B T_z / \mathrm{eV}}{m_z / \mathrm{u}}}$$

Magnetic field measurements

Magnetic fields split lines into their Zeeman components which gives, in principle, the magnetic field, if Doppler broadening does not dominate

$$\frac{\Delta\lambda^{split}}{\Delta\lambda_{1/2}} \mu \lambda_{pq} \frac{B}{(k_B T_z / m_z)^{1/2}}$$

This suggests to use long wavelength transitions (large λ_{pq}) in heavy ions (large m_z)

→ magnetic dipole transitions between fine structure level of the ground state

→ $2^2P \rightarrow 2^2S$ transition of injected high-energy Li-beams at 670.8 nm

Motional Stark effect

Fast beams (e.g. injected hydrogen heating beams) experience the Lorentz electric field

$$\vec{E} = \vec{v}_b \times \vec{B}$$

in their rest frame.

This gives a Stark-Zeeman pattern, where the Zeeman splitting can be smaller than the Stark splitting.

For diagnostics usually the Balmer-α line of hydrogen (deuterium) is employed. Excitation is primarily by *proton collisions* from the ground state.

Use is made also of the polarization characteristics

Early example

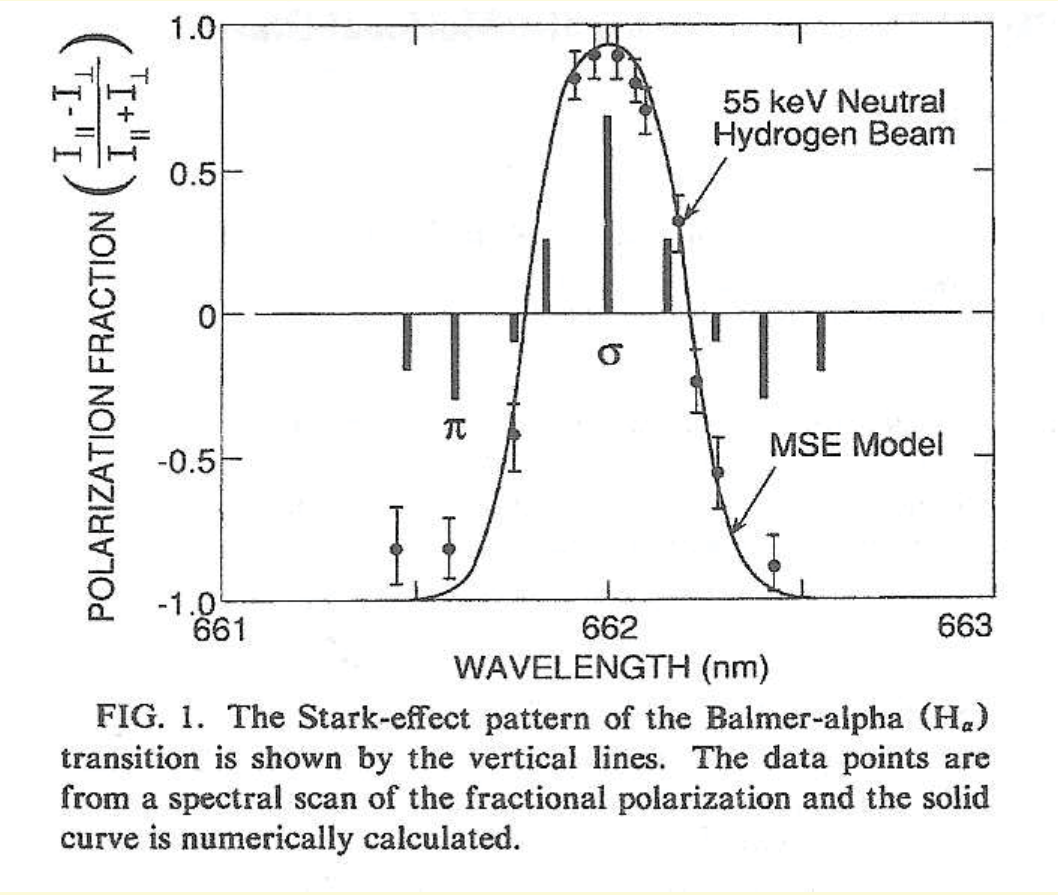

FIG. 1. The Stark-effect pattern of the Balmer-alpha (H_α) transition is shown by the vertical lines. The data points are from a spectral scan of the fractional polarization and the solid curve is numerically calculated.

Levinton et al. Phys. Rev. Lett. 63, 2060 (1989)

Some possible experimental mistakes, some of these are even found in publications

No accurate wavelength calibration of the spectrographic system,
people used only data from the manufacturer

A number of sources emitting well-known emission lines are available

No absolute spectral sensitivity calibration (authors simply used reflectivity data of grating and mirror, sensitivity of detector from manufacturer, area of entrance slit, solid angle),
Required is in most cases the calibration of the complete spectrographic system since alignment, imaging, solid angle, apertures, etc. influence the total sensitivity

From the infrared into vacuum-ultraviolet spectral region various primary and secondary standard are available

Difficulties with sources come up in the EUV and X-ray regions

here

Branching ratio method
employs two lines from
the same upper level

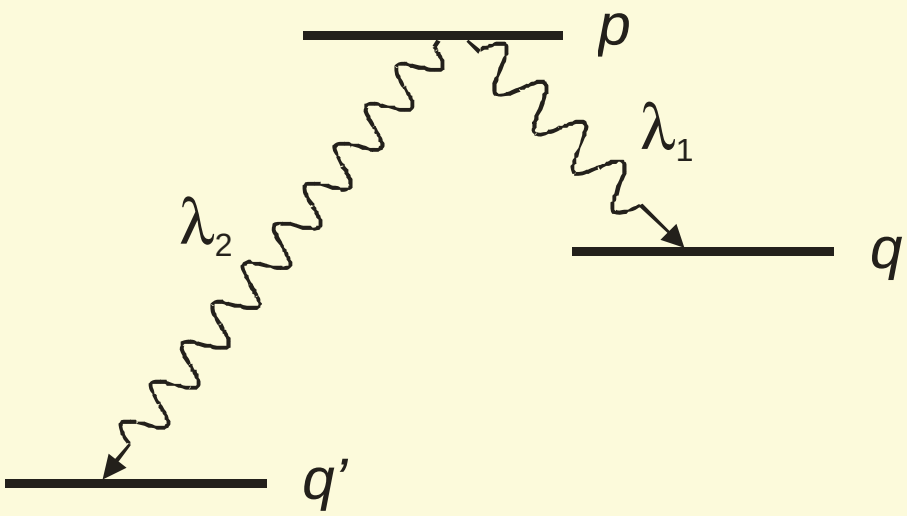

Calibration at long
wavelength (e.g. in the
visible) yields calibration
at short wavelength provided
Both transition probabilities A
are known with sufficient
accuracy

When studying two lines close in wavelength, no sensitivity calibration may be necessary

Transmission through air may have to be considered,
in some cases also transmission through optical components,
windows, lenses, filters

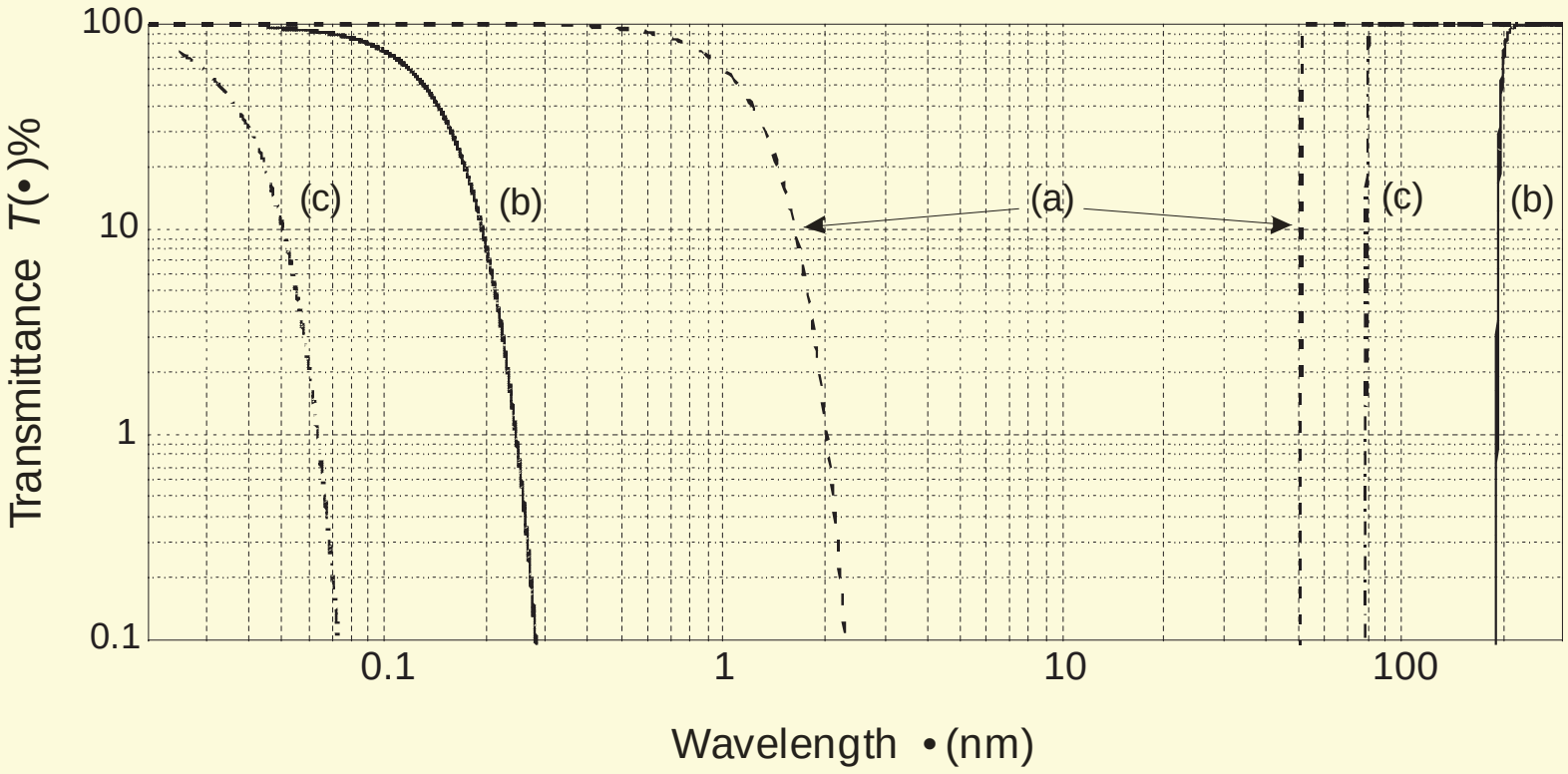

Transmission through 100 cm of gas at atmospheric pressure and at a temperature of 20°C: (a) He, (b) air, (c) Ar

In some spectral regions you have to work in vacuum !

Neglect of sensitivity change across a two-dimensional detector (pixel to pixel variation)

Irising effect in case of very fast gating a two-dimensional detectors due to finite travel time of gating pulse delay in switching from center to edge)

Vignetting in the optical path

No check of the optical thickness of spectral lines; authors even claimed as consequence of such wrong interpretation that the transition probability A changes at high electron densities. Several papers in top journal !

Saturation of detectors

Neglect of damping on fast signals in cables

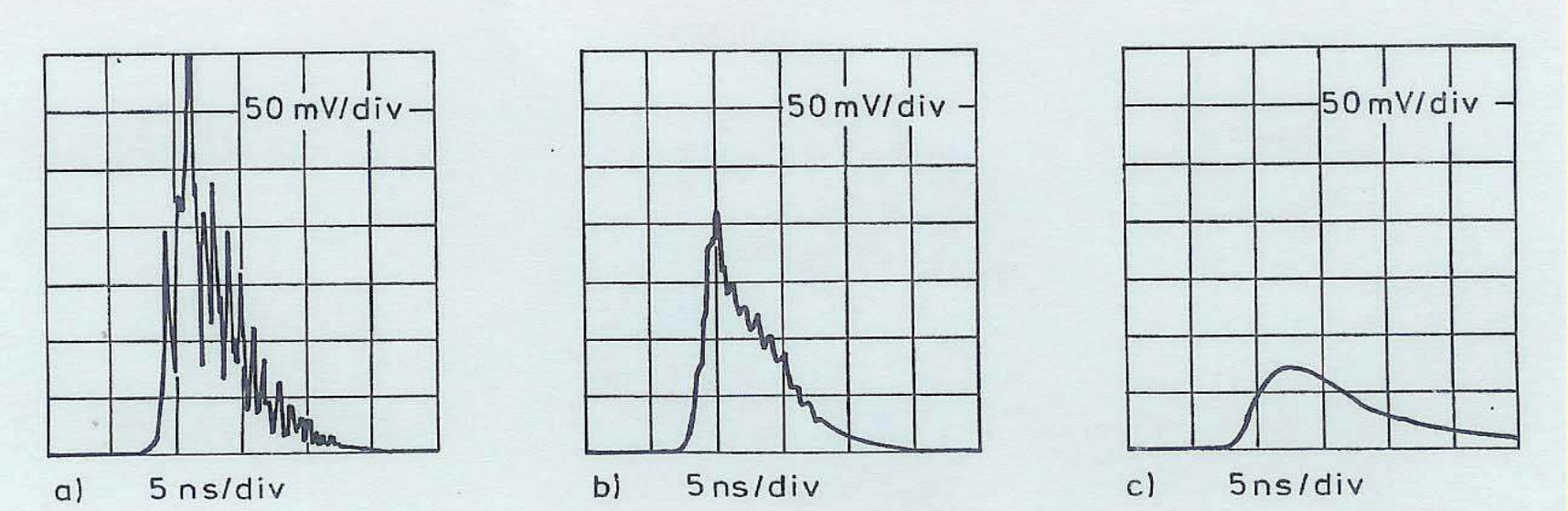

Signal from a photodiode recorded with a fast oscilloscope with a cable RG 58 C/U
a) 1 m long b) 11 m long c) 79 m long

Wrong interpretation of Rayleigh scattering signals from a ruby laser beam with varying pulse duration Δt

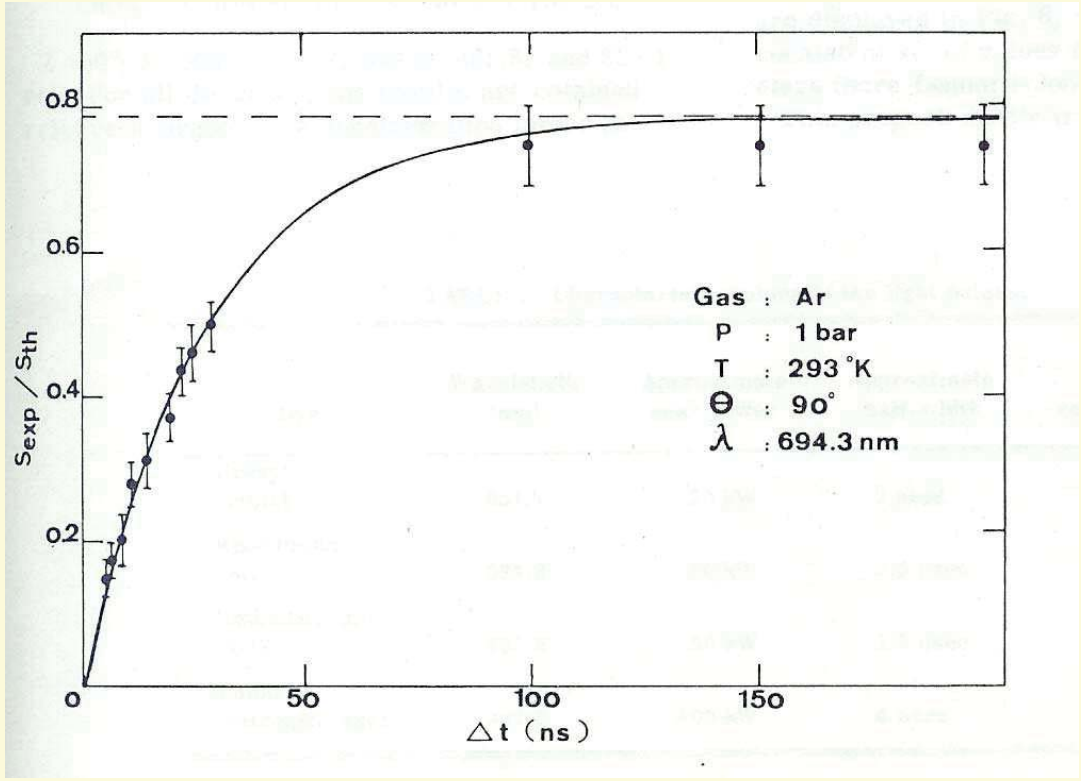

Phys. Rev. A **19**, 2260 (1978)

Use of a system outside its sensitivity/design range !

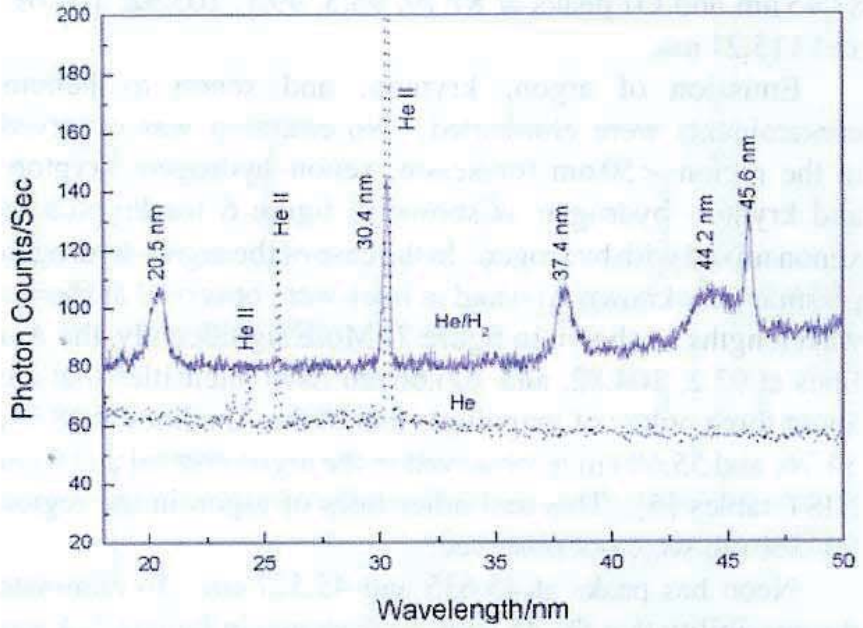

Figure 2. The EUV spectra (17.5–50 nm) of the microwave cell emission of the helium–hydrogen mixture (98/2%) (top curve) recorded at 20 Torr with a normal incidence EUV spectrometer and a CEM, and control helium (bottom curve) recorded at 20 Torr with a 4° grazing incidence EUV spectrometer and a CEM. Only known He I and He II peaks were observed with the helium control. Reproducible novel emission lines were observed at 45.6 and 30.4 nm with energies of $q \cdot 13.6$ eV, $q = 2$ or 3 (equations (2*a*) and (2*c*)) and at 37.4 and 20.5 nm with initial energies of $q \cdot 13.6$ eV. $q = 4$ or 6 that were inelastically scattered by helium atoms wherein 21.2 eV was absorbed in the excitation of He ($1s^2$) to He ($1s^1 2p^1$) as proposed in equation (8).

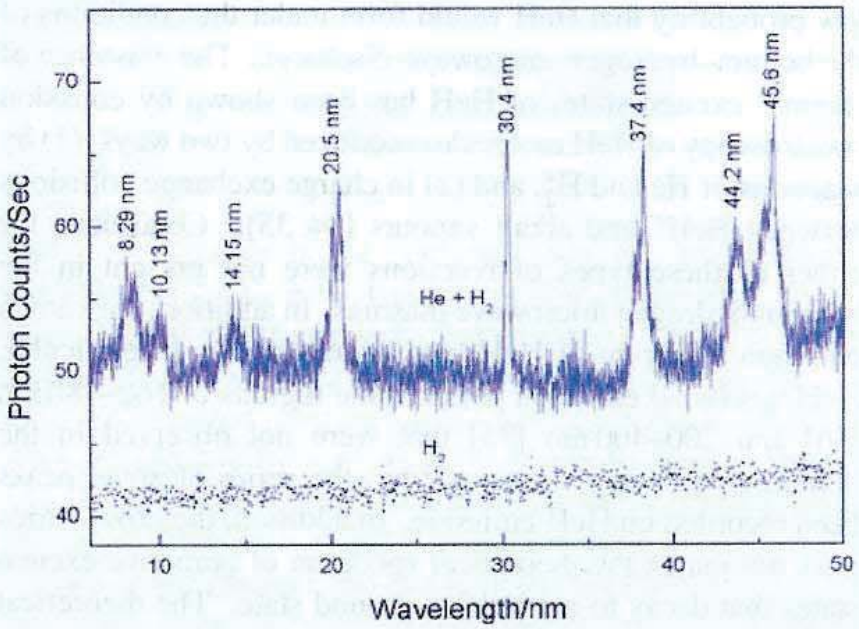

Figure 4. The short wavelength EUV spectra (5–50 nm) of the microwave cell emission of the helium–hydrogen mixture (98/2%) (top curve) and control hydrogen (bottom curve) recorded at 1 Torr with a normal incidence EUV spectrometer and a CEM. No hydrogen emission was observed in this region, and no instrument artefacts were observed. Reproducible novel emission lines were observed at 45.6, 30.4, 13.03, 10.13, and 8.29 nm with energies of $q \cdot 13.6$ eV, $q = 2, 3, 7, 9$, or 11 and at 37.4, 20.5 nm, and 14.15 nm with initial energies of $q \cdot 13.6$ eV, $q = 4, 6$, or 8 that were inelastically scattered by helium atoms wherein 21.2 eV was absorbed in the excitation of He ($1s^2$) to He ($1s^1 2p^1$) as proposed in equation (8). The peak at 13.03 nm was observed as a weak shoulder on the 14.15 nm peak, and has been observed in repeated (nonpresented) spectra.

Hydrino !!!

Some comments on spectrographic systems

Prism instruments are relatively easy to construct and to align and have no overlapping orders

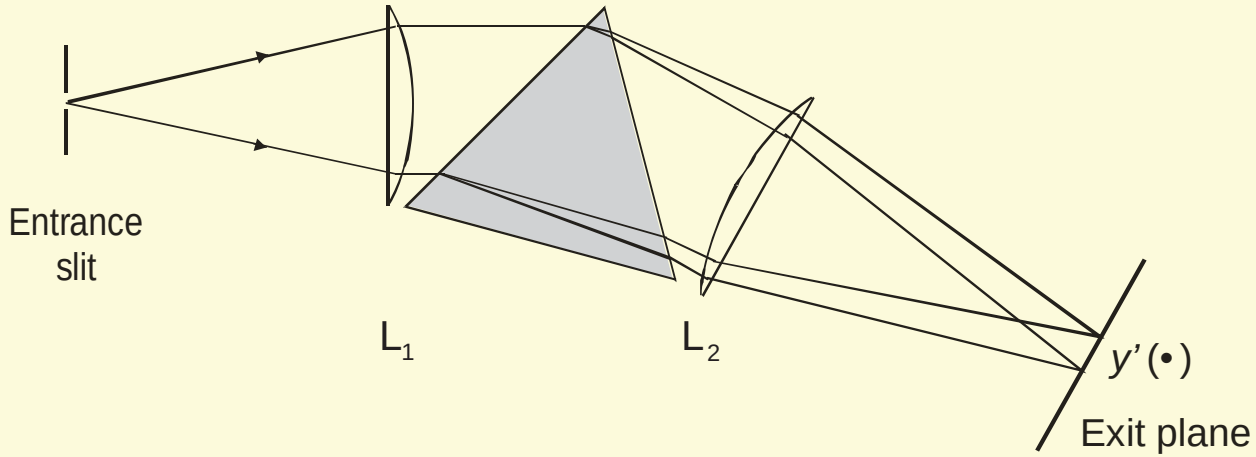

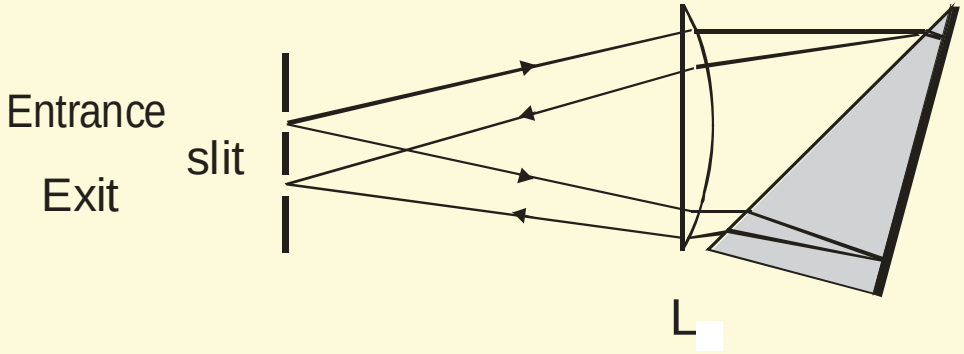

Littrow mounting

Instruments with gratings.

The most common mounting is the Czerny-Turner mount employing two mirrors;
They are off-axis spherical and properly tilted and coma can be canceled. Astigmatism is rather small as well.

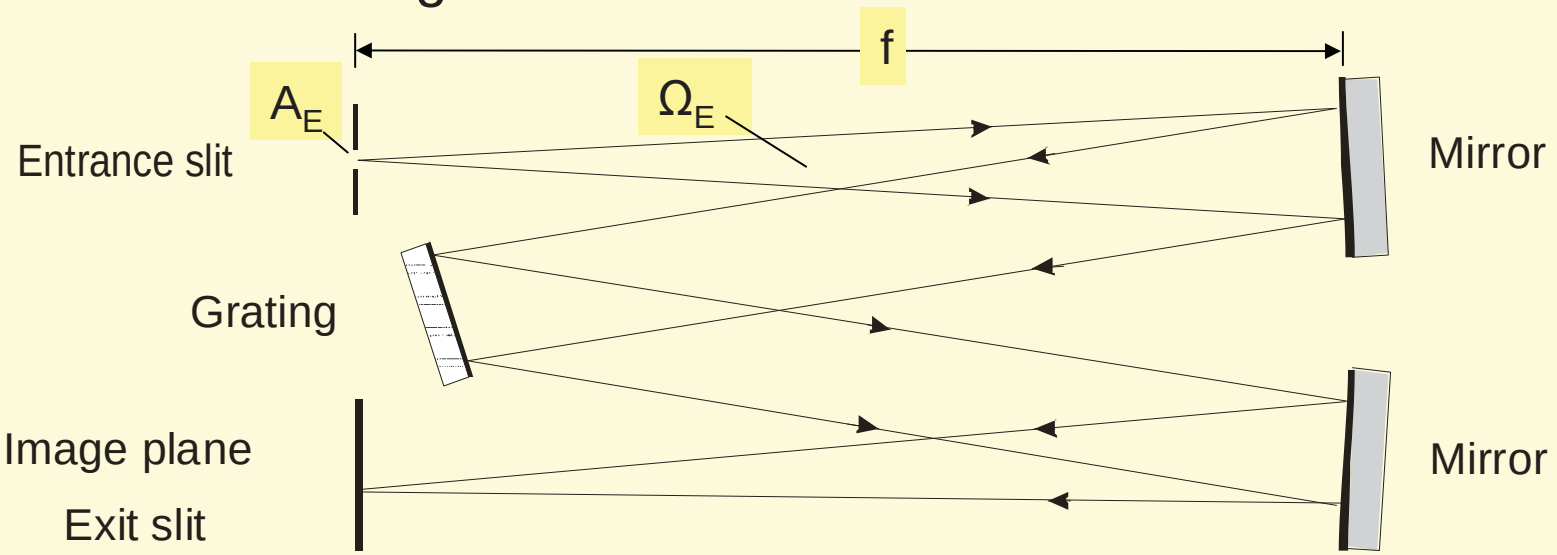

A very modern variant of this mounting employs an echelle grating close to the Littrow mount and allows high resolution in high orders. An additional prism separates orders.

It is obvious that the radiation flux entering the instrument is proportional to $A_E\Omega_E$,
where A_E is the area of the entrance slit and Ω_E is the solid angle,
$A_E\Omega_E$ is called throughput.

Since the width of the entrance slit E usually has to be small to obtaining reasonable spectral resolution (depending on the goal to measure total line intensities or line profiles), Ω_E is relevant for the maximum achievable flux.
Usual characterization of the radiation-collecting power by the so-called f-number f/D, where D is the dimension of the grating

With decreasing wavelength the reflectivity of the metal-coated mirrors and gratings decreases,
and the use of a single concave mirror becomes necessary, which combines both dispersion and focusing.
The standard concave grating is of spherical shape,
has, of course, strong astigmatism

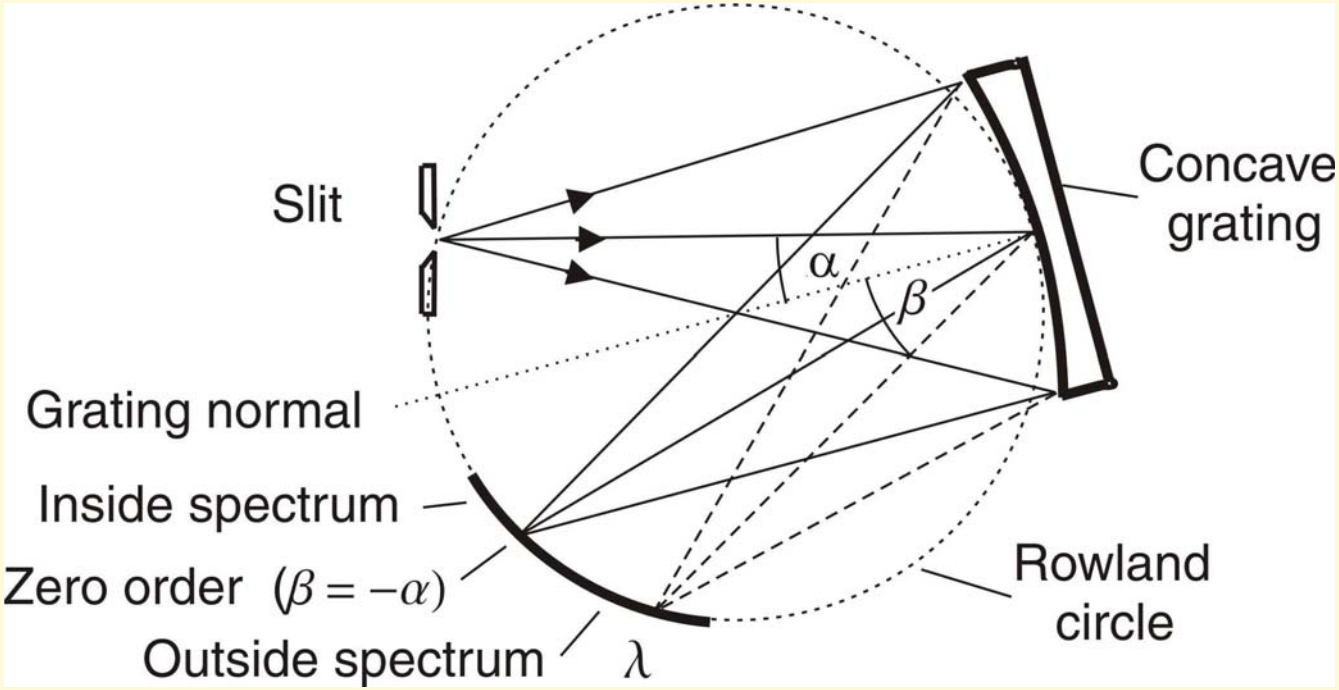

Grating of radius R
Rowland circle of radius R/2
entrance slit and grating positioned on Rowland circle
focusing is on this circle for all wavelength.

Nowadays, the above and other aberrations can be reduced, by employing toroidal gratings, variation of groove spacing and groove curving

The reflectivity of gratings is increased by going to small angles of incidence

→ grazing incidence mount

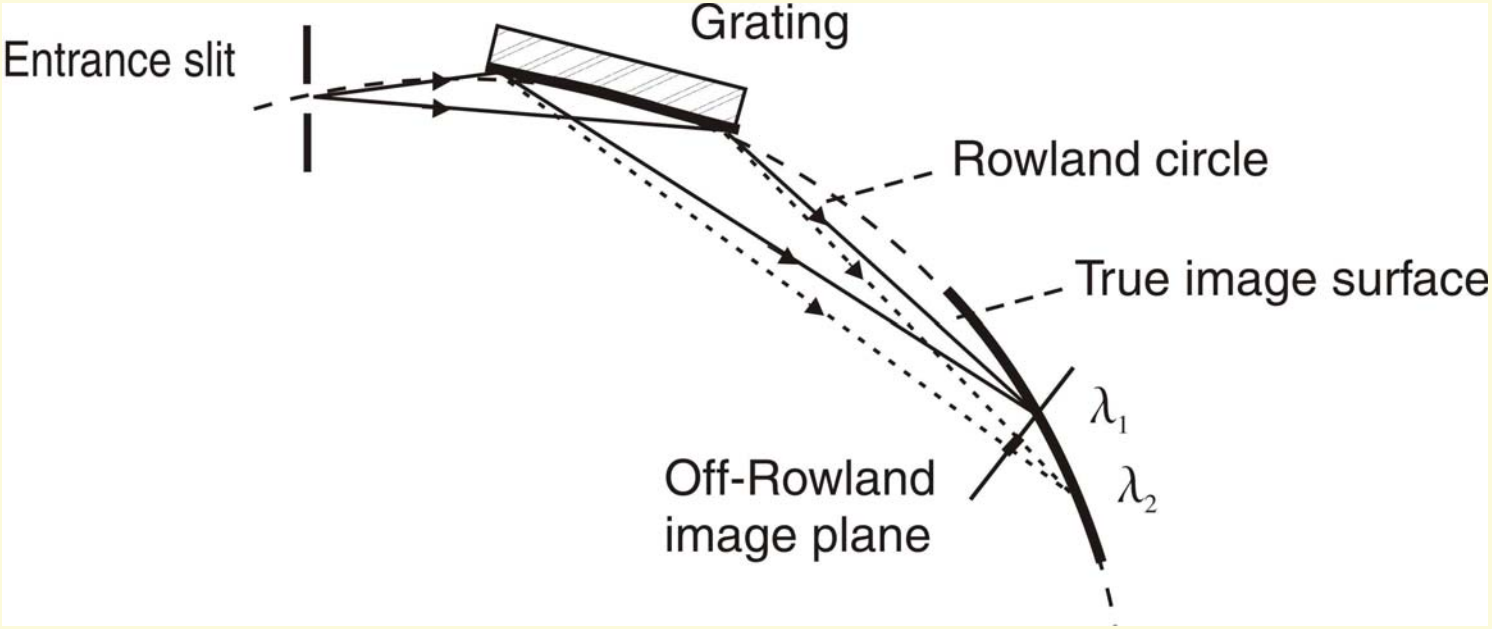

Wavelength range typically between 1.5 and 100 nm

Varying line spacing → focal surface is flat !!

Such flat-field instruments are very compact

Spectroscopy at wavelength, say shorter than 1.5 nm, requires crystals as dispersing elements.

Radiation scattered coherently at the atoms of a crystal interfere constructively only for one direction given by the famous

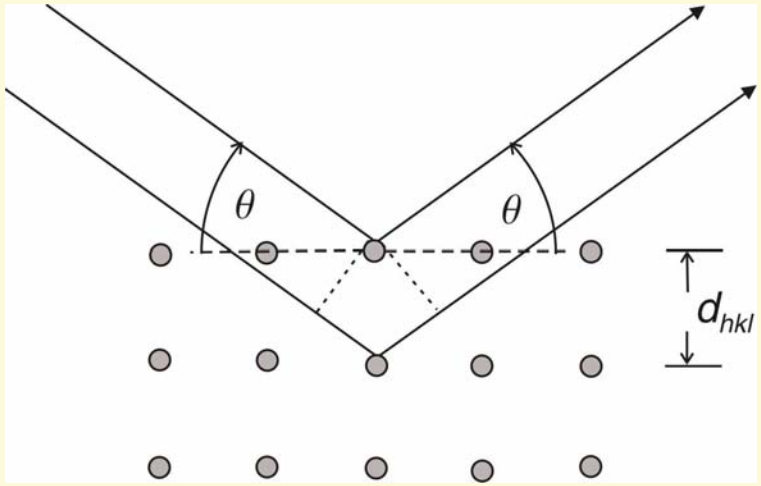

Bragg condition

$$m\lambda = 2d_{hkl}\sin\theta$$

Selection of the crystal spacing d_{hkl} fixes the relation between • and Bragg angle θ

Reflection from a plane crystal
Radiation forms a cone for each wavelength

Spectral lines on a plane detector
are thus sections of a circle,
an ellipse, a parabola or a hyperbola

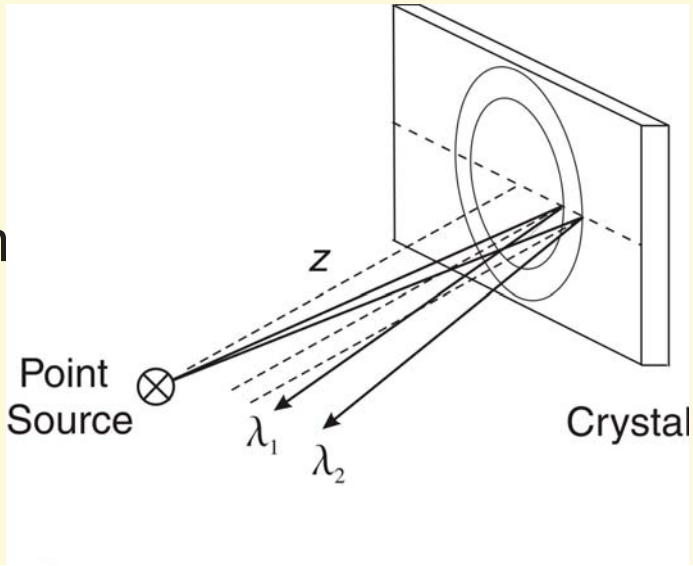

Curved crystals focus like spherical gratings employing also the Rowland mount

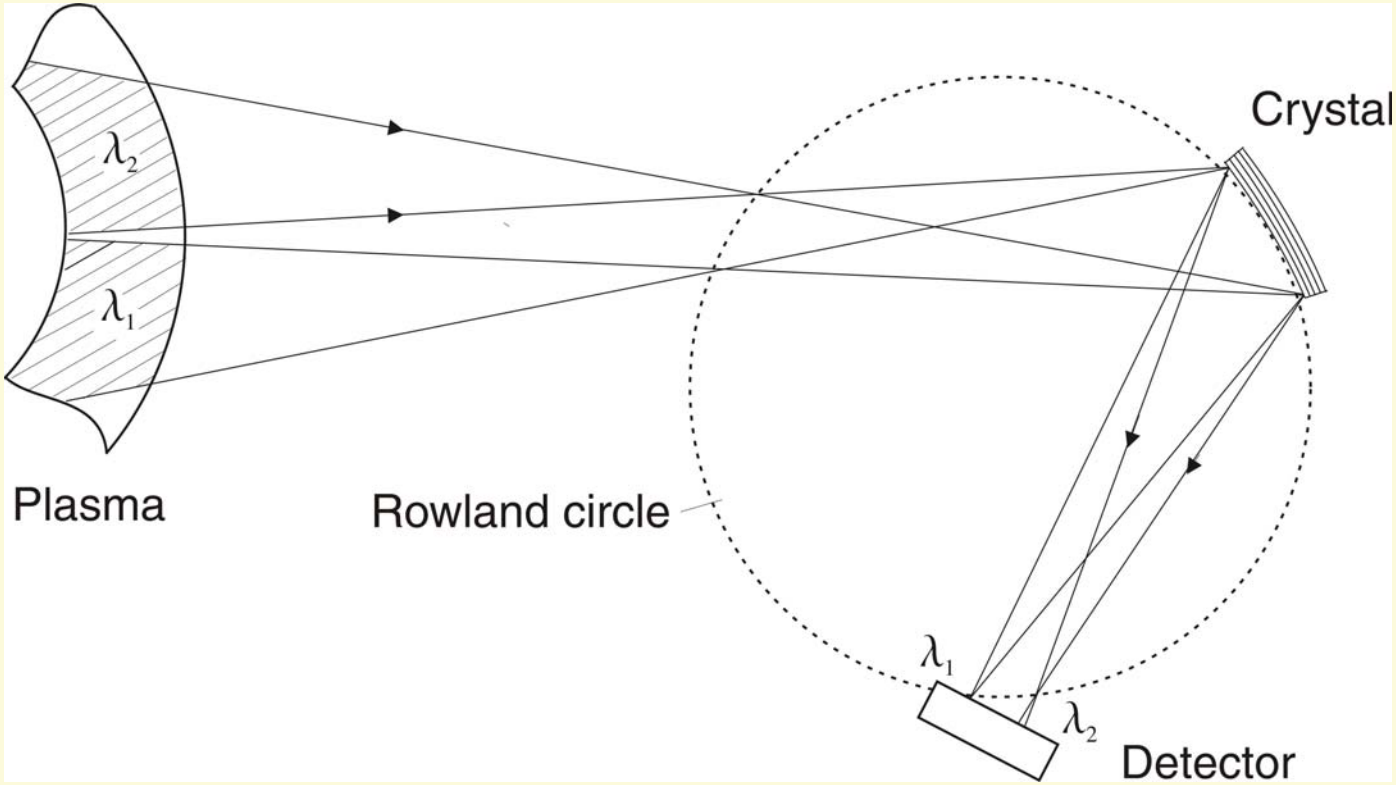

Here we see a mount used on large tokamaks. The plasma is outside the Rowland circle

Examples of other mounts are:

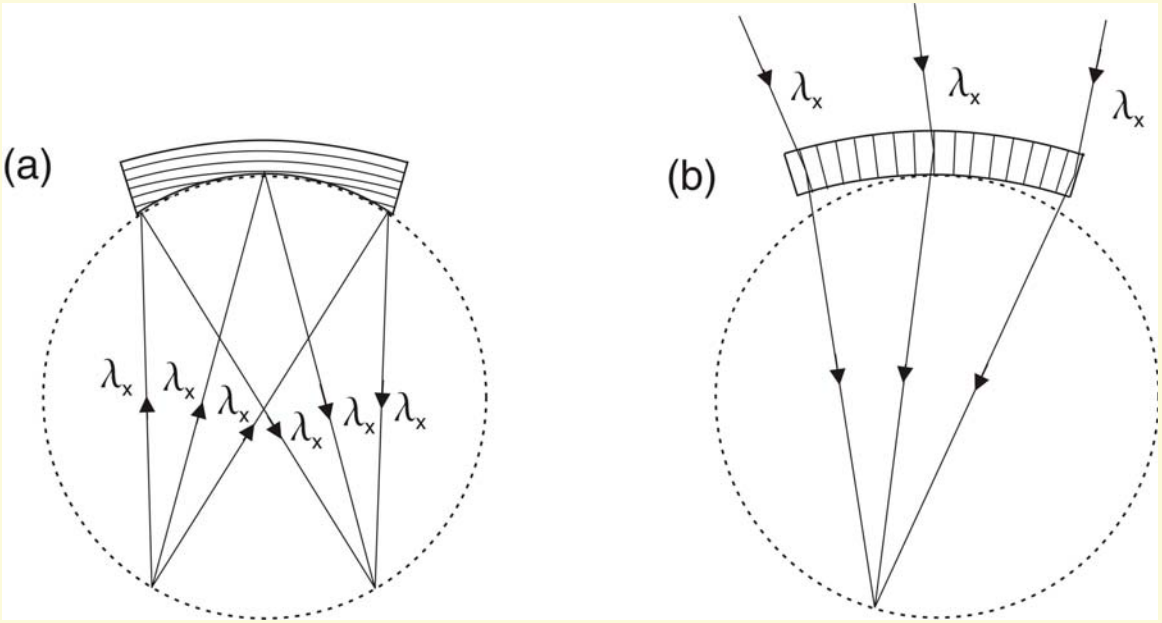

Johansson

Cauchois mount

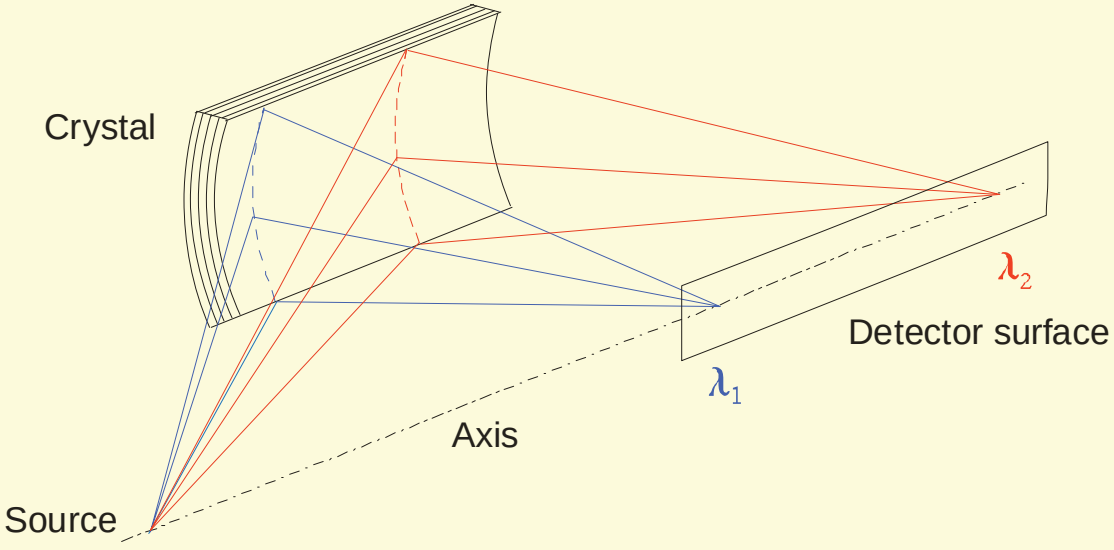

Van Hamos mount employs a cylindrically bent crystal

A very simple method the determination of the electron temperature provides the two foils method

One detects the radiation transmitted through two thin metallic foils of the same metal but of different thickness or of different metals:

long wavelength radiation is absorbed

short wavelength radiation is transmitted and detected

The ratio of the radiation transmitted through properly selected foils is a strong function of the electron temperature T_e. It is usually very convenient for plasma above 100 eV.
One must be sure that there is no line radiation !

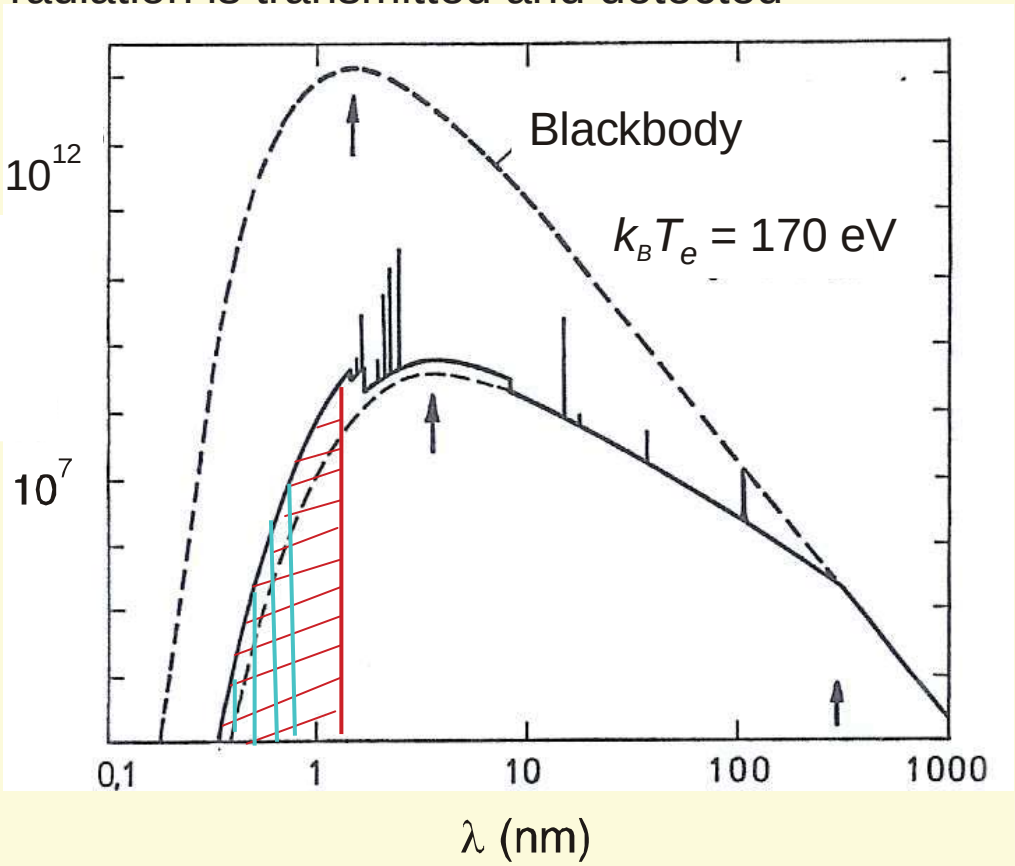

Transmission curves: http://www.-cxro.lbl.gov/optical_constantsfilter2.html

How do you get started with the spectroscopic investigation of a plasma?

First you must estimate the temperature range you expect the plasma to have, since this determines the optimal spectral range of line emission and thus the type of instrument needed.

Each element has a specific spectrum for each ionization stage but the spectra of ions along an isoelectronic sequence show similarities which change slowly with Z.

The spectra emitted by the working gas, which you know, are usually the ones you will use and analyze to obtain the plasma parameters.

In fusion plasma, where the working gas is deuterium, impurity species from the walls are utilized, in other plasmas small amounts of impurities may be injected simply for diagnostic purposes.

The selection of the detector in the exit plane of the instrument depends on

Do you want to record a spectrum at several times during the life time of the plasma?

You probably select a gated CCD camera and repeat the measurement at different times or for very short-lived plasmas you use a fast streak camera

or Do you want to record the time evolution of single lines?

You employ photomultipliers or photodiodes behind an exit slit or even behind multiple slits, maybe by using optical fibers

Now you have to collect the relevant atomic data A, X, S, α

Although the available data collected in data centers are steadily growing, the shortage is still large.
One continuously has to search the new literature

Collisional radiative models of varying complexity have been setup by several groups and are reported in the literature.

An extremely useful tool is provided by the FLYCHK code.
It is maintained by National Institute of Science and Technology, NIST.
It can be used interactively on the internet
http://physics.nist.gov/PhysRefData/contents.html

Lecture is based on

Introduction to Plasma Spectroscopy
H.-J. Kunze
Springer, Heidelberg, 2009